DRAFT BRUKER XRF SPECTROSCOPY USER GUIDE:

SPECTRAL INTERPRETATION AND SOURCES OF INTERFERENCE

TABLE OF CONTENTS

TABLE OF CONTENTS 1

ABSTRACT 3

XRF THEORY 4

INSTRUMENTATION 6

- **ED-XRF EQUIPMENT** 6
- **TRACER** 8
- **SI PIN DIODE DETECTOR PARAMETERS** 8
- **ARTAX** 9
- **SI(LI) SDD DETECTOR PARAMETERS** 9

SPECTRAL INTERPRETATION 9

INTERACTIONS IN THE DETECTOR 11

- **SUM PEAKS** 11
- **ESCAPE PEAKS** 12
- **ESCAPE PEAKS (CONTINUED)** ERROR! BOOKMARK NOT DEFINED.
- **HETEROGENEITY** 15
- **HETEROGENEITY (CONTINUED)** 16

INTERFERENCE WITH INSTRUMENTATION 17

- **EQUIPMENT AND INSTRUMENT CONTRIBUTION** 17
- **EQUIPMENT AND INSTRUMENT CONTRIBUTION (CONTINUED)** 18
- **THIN FILM ANALYSIS (BACKGROUND CONTRIBUTION)** 19

THIN FILM ANALYSIS (BACKGROUND CONTRIBUTION) ERROR! BOOKMARK NOT DEFINED.

PHENOMENA IN THE SAMPLE **20**

RAYLEIGH (ELASTIC) SCATTERING **20**
RAYLEIGH (ELASTIC) SCATTERING (CONTINUED) **21**
COMPTON (INELASTIC) SCATTERING **22**
MATRIX EFFECTS **23**
BRAGG SCATTERING **24**
BRAGG SCATTERING (CONTINUED) ERROR! BOOKMARK NOT DEFINED.
BRAGG SCATTERING (NIST C 1122 EXAMPLES) **26**
BRAGG SCATTERING (GEMSTONE EXAMPLES) ERROR! BOOKMARK NOT DEFINED.
BRAGG SCATTERING (GEMSTONE EXAMPLES) ERROR! BOOKMARK NOT DEFINED.

SIX FIELD APPLICATIONS **28**

IDENTIFYING GENUINE ARTIFACTS (CHELSEA BULLFINCH EXAMPLE) **28**
IDENTIFYING TRUE ORIGINS (STONEWARE EXAMPLE) **29**
MEASURING CHLORINE WITH THE TRACER AND OTHER FIELD APPLICATIONS **30**

APPENDICES **41**

APPENDIX A **43**
APPENDIX B **48**
APPENDIX C **49**
APPENDIX D **50**
APPENDIX E **51**

By Dr Bruce Kaiser and Alex Wright

November 11, 2008

ABSTRACT

While performing XRF spectroscopy, three main factors contribute to the analytical spectrum: interactions in the detector, interference with the instrumentation, and phenomena in the sample. This user guide to ED-XRF provides a basic outlining of the physics involved in XRF spectroscopy, an overview of the main components of the Bruker TRACeR and ARTAX units, as well as a delineation, explanation, and resolution of the several phenomena included in performing XRF spectroscopy. Each section includes a textual explanation of why it occurs and how it affects a spectrum, as well as example spectra that clearly identify the phenomena. Several field applications and examples are provided, as well as an appendix with additional information

XRF THEORY

General Concept Behind X-Ray Fluorescence Spectroscopy

Every element has a characteristic electron structure. When inner shell electrons are ejected from an atom, electrons from shells with less binding energy fill the holes and may release x ray radiation equivalent to the difference in energy between the level the electrons came from to that which they went. The x ray radiation released during these transitions is characteristic to the element and has a specific energy (± 2 eV) depending on the transition made within the atom. By bombarding a sample with radiation that exceeds the binding energy of the electrons in the atoms of which the material is composed of and detecting the energy and number of resultant characteristic x rays emitted from each element, it is possible to determine the composition and proportional concentrations of those elements.

Two common methods of X-ray spectroscopy exist: Wavelength Dispersive XRF (WD-XRF) and Energy Dispersive XRF (ED-XRF). The main difference between the two methods is how the emitted x rays are measured; WD-XRF uses an analyzing crystal to diffract the different x ray wavelengths and detectors are placed at the various angles to measure the number x rays diffracted at each angle. A single detector maybe used to measure all the various energies if one moves the detector to cover all the angles, because each energy comes out of the crystal at a different angle.

Energy dispersive x ray fluorescence (ED-XRF) uses a detector that collects x rays of all energies and sorts out each x ray energy by the amount of electrons each x ray knocks free in the detector lattice, typically silicon. The number of electrons knocked free depends on the in coming x ray energy and the particular interaction that that x ray has with the material lattice. To accurately determine the x ray energy all the electrons from each event that occurs in the detector must all be collected and converted ultimately to a digital signal. Thus the detector measures one x ray at a time.

Bremsstrahlung Radiation

In most xrf systems the beam of x rays incident on the sample are produced with a vacuum tube and created by bombarding a target (such as Rh, W, Cu, or Mo) with highly accelerated electrons. Shown in Figure 1, as the electrons penetrate the target atoms, they may have their direction changed as they pass near the nucleus of the target atoms causing a sudden deceleration and loss of kinetic energy. In this loss of kinetic energy the electron may emit an x ray with energy related to the amount of energy lost. As a result a broad spectrum of x ray energies, known as a Bremsstrahlung continuum, is

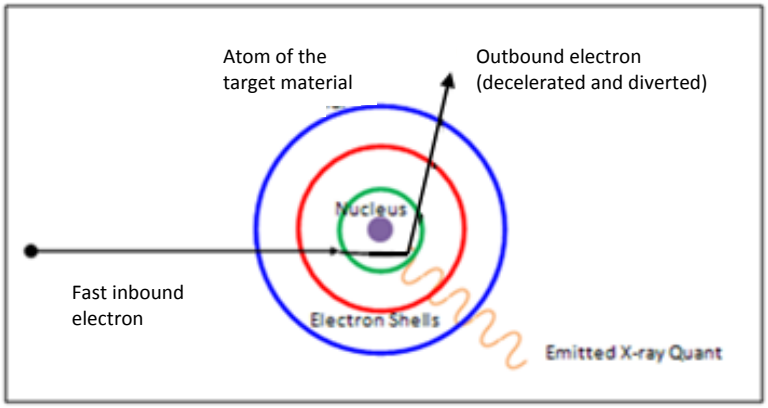

Figure 1: Diagram of the Bremsstrahlung effect

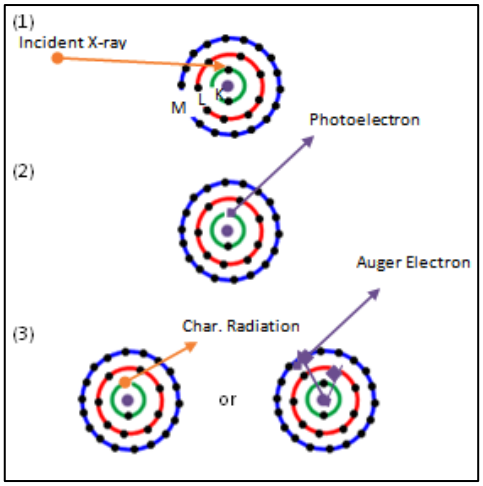

Figure 2: Diagram of possible excitation routes

emitted from the x ray tube target. This continuum can be adjusted by tube high voltage settings, beam filtering and secondary targets to allow one to focus on detection of specific elements with in the sample. This capitalizes on the different absorption edges of each element. The accelerated electrons also cause the target to fluoresce. These target characteristic x rays are also incident on the sample, and must be considered during data analysis

The Photoelectric Effect and Inner Shell Ionization

When an x ray interacts with an atom several different reactions can occur depending on the x ray's energy. Low energy photons, such as a light waves, can excite and eject outer shell electrons from the atom and excite inner shell electrons to higher energy levels. X rays can eject inner shell electrons from the atom, creating a vacancy in the inner shell and put the atom in an unstable condition, providing the that incoming x ray has an energy which exceeds the binding energy of the electron it interacts with. When a vacancy is created, the atom quickly relaxes (less than 10^{-7} s) by transitioning an electron from a higher shell to the vacancy. During this transition an x ray with the energy equal to the energy difference of the transition maybe released. This x ray is known as a characteristic x ray and is specific to the transition and element in which it occurs. Figure 2 illustrates the different interactions that can occur when x rays interact with the bound electrons of an atom. Once the characteristic x rays are created, they may escape the atom and the matrix material at random angles and a very small fraction enter the detector. If geometry, density and other factors are known, the number of x rays entering the detector can be related to the type and number of atoms present in the sample.

Table 1: Possible electron locations in an atom

Shell (number of electrons)	n	ℓ	m	s	Orbitals	J
K (2)	1	0	0	±½	1s	½
L (8)	2	0	0	±½	2s	½
	2	1	1	±½	2p	½, 3/2
	2	1	0	±½	2p	½, 3/2
	2	1	-1	±½	2p	½, 3/2
M (18)	3	0	0	±½	3s	½
	3	1	1	±½	3p	½, 3/2
	3	1	0	±½	3p	½, 3/2
	3	1	-1	±½	3p	½, 3/2
	3	2	2	±½	3d	3/2, 5/2
	3	2	1	±½	3d	3/2, 5/2
	3	2	0	±½	3d	3/2, 5/2
	3	2	-1	±½	3d	3/2, 5/2
	3	2	-2	±½	3d	3/2, 5/2

Characteristic Lines

The energy of the x ray released by the relaxation of an ionized atom is dependent on the element from which it came, the location of the vacancy, and the electron that fills the vacancy. Electrons exist in quantized energy levels; they are not free to roam anywhere around the nucleus of the atom. A given electron is located in a given electron shell using the quantum numbers *n, l, m, s*, where n indicates the shell, l indicates the sub-shell, m_l indicates the energy shift within the sub-

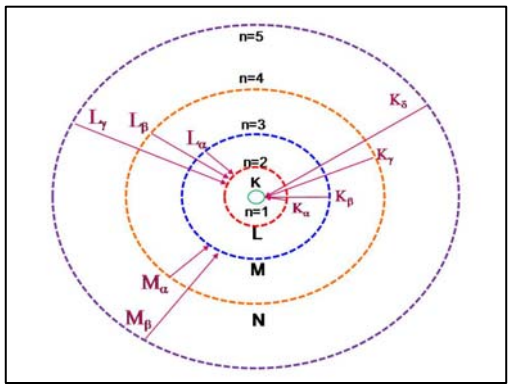

Table 2: Example of possible transition notations for a Barium atom.

Line	Siegbahn	Electron Binding Energies (keV)	Energy of emitted radiation (keV)	Wavelength (Å)
$K\text{-}L_2$	$K\alpha_2$	37.441.5 634	31.80	0.390
$K\text{-}L_3$	$K\alpha_1$	37.441.5 247	32.194	0.385
$K\text{-}M_2$	$K\beta_3$	37.441.1 137	36.304	0.342
$K\text{-}M_3$	$K\beta_1$	37.441.1 062	36.379	0.341
$K\text{-}N_2$	$K\beta'_5$	37.441.0 192	37.249	0.333
$K\text{-}N_3$	$K\beta''_5$	37.441.0 180	37.261	0.333
$L_3\text{-}M_1$	L_1	5.247.1 293	3.954	3.136
$L_3\text{-}M_4$	$L\alpha_2$	5.247.0.796	4.451	2.786

shell, and m_s indicates the spin of the electron. Table 1 lists some of the possibilities for electron locations in an atom. There are a couple ways of describing an x ray of a certain transition. It can be written in Line notation, Siegbahn notation, or described by the characteristic energy or wavelength connected that x ray. These notations are shown below in Table 2 with an example of Barium electron transitions. In the Siegbahn notation, the Greek subscript denotes the probability of the transition (intensity), proceeding from the most to least (α, β, γ, etc.).

INSTRUMENTATION

The TRACeR and ARTAX are both ED-XRF units with Silicon based detectors. The TRACeR is a handheld unit commercially offered by Bruker AXS and provides for quick and easy qualitative analysis and chemistries for elements as low as Mg. The Tracer handheld XRF analyzer provides spectral analysis through PXRF analytical software. The instrument's high sensitivity allows the user to identify the elements in a sample matrix, with concentrations as low as ppm. The PXRF software program provides qualitative and quantitative analysis, in addition to the voltage and current control of the X-ray tube, which makes possible a wider range of elemental analysis. The ARTAX is the first commercially available, portable micro-XRF spectrometer designed to meet the requirements for a spectroscopic analysis of unique and valuable objects on site, i.e. in archeometry and art history. The system performs a simultaneous multi element analysis in the element range from Na(11) to U(92) and reaches a spatial resolution of down to 30 µm. Both instruments allow one to utilize filters and secondary target to adjust the incident x ray beam in both energy distribution and intensity.

ED-XRF EQUIPMENT

The ARTAX and TRACeR systems have several separate components that all serve their own function in the process of recording X-ray fluorescence. The main components in terms of functionality are the X-ray tube system, collimators, filters, detector and signal processing hardware and software. The ARTAX and the TRACeR Turbo are very similar in functionality. Both units employ energy dispersive technology and a Silicon based detector. Being a handheld unit, the TRACeR is battery operated, more convenient, but has a beam spot size of 3 by 4 mm (much larger than the Artax). The ARTAX is portable; however, it is not generally used in the field like the battery operated handheld TRACeR unit. Both units can use a variety of changeable filters, tube voltage and current settings making them uniquely capable of being configured to maximize their sensitivity to specific elements of interest.

X-ray Tube: Electrons are generated and accelerated to high speeds and then bombarded a target usually composed of a pure metal (e.g. W, Mo, Cr, or Rh). Upon reaching the target the electrons either interact and ionize the target, creating characteristic x-rays, or are decelerated upon nearing the nuclei, creating a Bremsstrahlung continuum. Figure 4 illustrates the production of the X-Ray beam.

Figure 4: Diagram of an end window x-ray tube

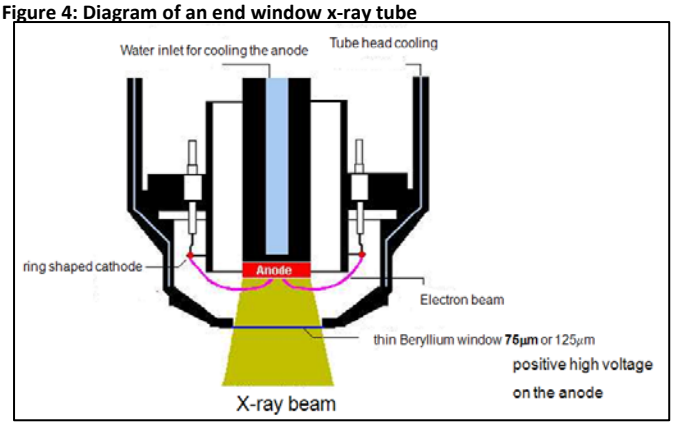

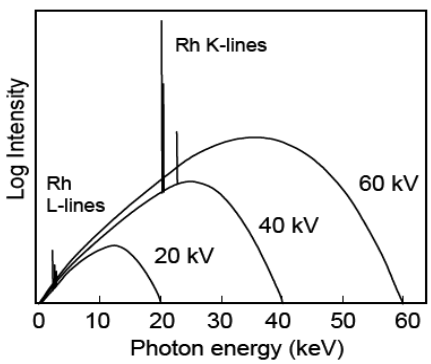

Figure 6: Emission spectra of an Rh target X-ray tube run at three different voltages

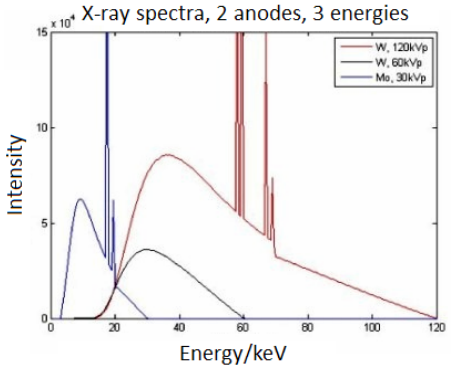

Figure 5: Overlapping emission spectra of W and Mo target X-ray tubes run at different voltages

Filter: A filter can be placed between the tube and the sample to remove undesirable background radiation below a certain voltage. The level of radiation filtered out is dependent on the filter element composition and its thickness. Table 3 suggests some filter types for certain applicatons and Appendix A provides a list of others for the TRACeR and ARTAX units, as well as other filter information. Note both units allow the user to fabricate any filter or secondary target they think is best for their application.

Filter	Thickness	kV range	Elements
No filter	N/A	4-50	All, Na-Ca
Cellulose	Single sheet	5-10	Si-Ti
Thin aluminum	25-75 µm	8-12	S-V
Thick aluminum	75-200 µm	10-20	Ca-Cu
Thin anode element	25-75 µm	25-40	Ca-Mo
Thick anode element	100-150 µm	40-50	Cu-Mo
Copper	200-500 µm	50	>Fe

Table 3: Available filters that can be used with the ARTAX and TRACeR units

Collimator: Collimators are usually circular or a slit and restrict the size or shape of the source beam for exciting small areas. Collimator sizes range from 12 microns to several mm. Figure 7 illustrates the general function of a collimator.

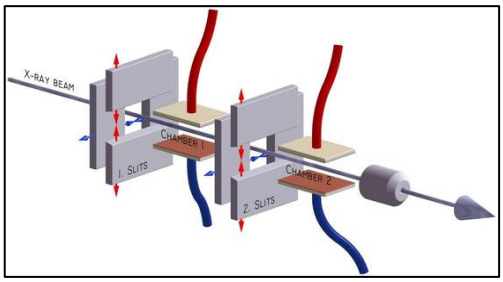

Figure 7: X-ray passing through a collimator

Detector: The detector is used to convert incoming x-rays into proportionally sized analog pulses that are then converted by a digital pulse processing system to information that can be read by a computer and displayed on a spectrum. The resolution of the detector depends on the type and quality of the detector (see Figure 8).

Figure 8: Graph comparing the resolution of several different types of detectors

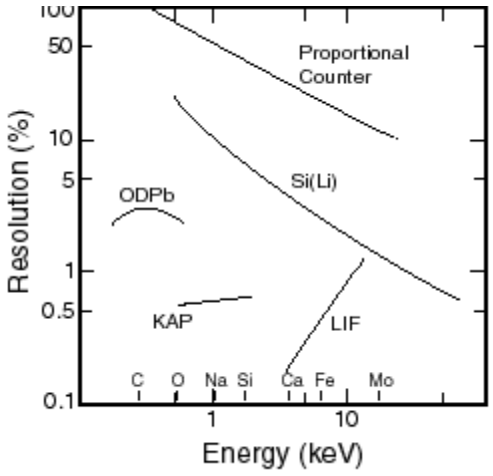

TRACeR

The TRACeR is a handheld ED-XRF unit used for instant nondestructive elemental analysis anywhere, anytime. It can be used in a wide range of applications including elemental analysis in material research, archeological digs, museum artifact analysis, conservation and restoration, electric utility industry, engine assembly, airframe assembly, scrap industry, metal producers, foundries, and maintenance assessment, and many other applications.

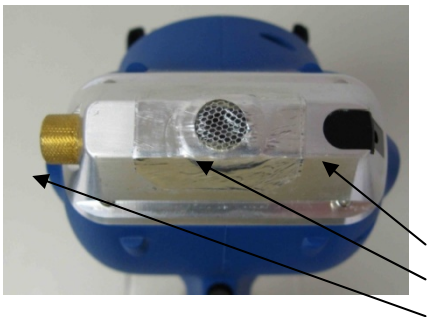

Figure 9: Front view of the TRACeR unit

- X-ray tube (typically Ag, Rh or Re Target)
- Up to 45kV X-rays
- 170eV Si PIN or 145eV SDD
- 13µ Be Detector Window
- IR Safety Sensor
- Vacuum window
- User selectable filter/target
- Up to 200 kcps (SDD)

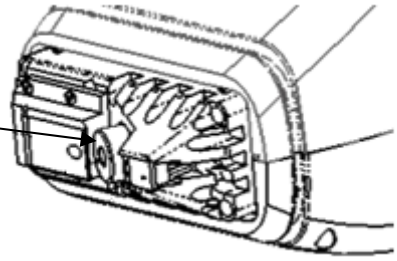

Figure 10: Sketch of TRACeR module

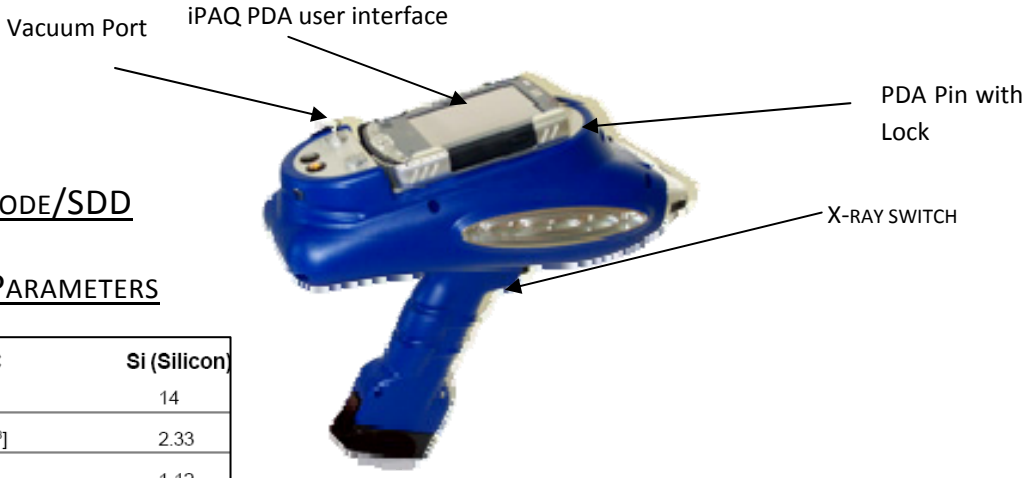

Si PIN Diode/SDD

Detector Parameters

CHARACTERISTIC	Si (Silicon)
Atomic Number, Z	14
[1]Specific Density, [g/cm³]	2.33
[2]Band Gap, [eV]	1.12
[3]Melting Point, [°C]	1412
[4]Hardness, [Brinell]	1150
[5]Energy/Pair, [eV]	3.62
[6]Resistivity	10^4
[7]Mobility, [cm2/(Vsec)]	
electrons:	1400
holes:	480

Table 4: Si PIN/SDD characteristics (see Appendix B for explanations)

X-ray Tube	Ag, Rh, or Re
Filter	Selectable (See Appendix A)
Voltage Selection	Variable, 0-45 kV
Current Selection	Variable, 0-60 µA
Scan Length	Selectable
Optimal Pulse Density	15,000 max cps (PIN), 150,000 (max cps (SDD)
Environment	Air or Vacuum
Detector Channels	1023 PIN/2048 SDD

Table 5: TRACeR operating parameters

ARTAX

The ARTAX unit is a semi-portable open beam ED-XRF machine used for non-destructive elemental analysis of surfaces and the spectral mapping of surface areas within minutes. It may be used in many applications such as in archeometry, art history, restoration, forensic sciences, process related quality control, and material sciences. Appendix C includes a complete table of technical parameters for the ARTAX unit.

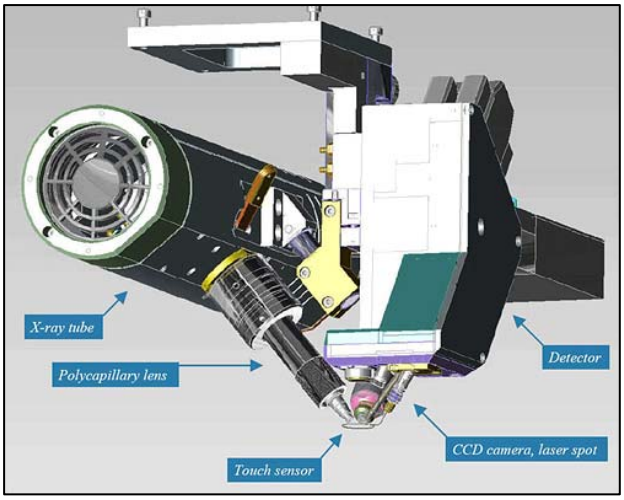

Figure 11: ARTAX model with labeled parts

- Mo, W, Rh, or Cr, Cu, Ti X-ray tube
- Up to 50 kV
- Less than 155 eV resolution Si(Li) SDD Detector
- Collimator
- Changeable Filter
- More than 100 kcps

Si(Li) SDD Detector Parameters

Parameter	Value
Energy range, keV	1 - 60
Detector sensitive area, mm^2	20 *
Energy resolution for 20 mm^2 sensitive area detector, eV at energy 5.9 keV 59.6 keV	 180 450
Integral nonlinearity , %	< 0.05
peak / background ratio	≥ 2500
Time instability during 8 hours of continuous work, %	< 0.05
Input count rate, pulse/sec	1.5×10^5
Dimensions of detection unit, mm	Ø 90 x 210
Dimensions of spectrometric device Multispectrum	300 x 180 x 80
Weight of detection unit, kg	2
Weight of spectrometric device Multispectrum, kg	2.8
Consumed power, W	100
Power Supply, V	220
Frequency, Hz	50

Table 6: Table of Si(Li) detector parameters

X-ray Tube	Mo, W, Rh, Cr, or Cu
Filter	Selectable (See Appendix A)
Voltage Selection	0-50 kV
Current Selection	0-1000 µA
Scan Time	Variable
Optimal Pulse Density	<50,000 cps
Environment	Air or Helium Flush
Detector Channels	4096

Table 7: ARTAX operating parameters

Spectral Interpretation

Although the goal of XRF spectroscopy is generally to elementally analyze the sample, several phenomena inherent from x ray physics involved contribute to the spectra. These influences require interpretation in order to correctly understand the data (see Figure 12). Three main influences contribute to the output spectra of a sample: interactions in the detector, x rays contributed by the analysis system, and x ray interactions in the sample. These interactions are delineated below and discussed in detail later in the document.

- Interactions in the Detector
  - Sum peaks- Interpretation of two or more pulses as one

- Escape peaks- Partial Loss of energy due to fluorescence in matrix (Si) detector
- Compton scattering- Partial loss of x ray energy entering detector
- Heterogeneity- Overlapping peaks due to detector resolution

- x rays contributed by interactions in the analysis system
  - X-ray tube target characteristic lines- Rayleigh scattered into the detector
  - Detector can lines- Iron and Nickel trace peaks
  - Window lines- Calcium trace peaks
  - Collimator and instrument structure lines- Aluminum trace peaks
  - Thin Film Analysis- Detection of surface below sample

- Phenomena in the Sample
  - Rayleigh scattering (elastic collisions)- No loss of x ray energy
  - Compton scattering (inelastic collisions)- Partial loss of x ray energy in the sample
  - Matrix effects- Misrepresentation due to secondary absorption/excitation, density effects
  - Bragg scattering- Constructive interference of X-rays in lattice structures

The ATRAX and TRACeR units have the option to change the voltage, current, and filter selection, and the use of a secondary target to specify the most efficient parameters for a given sample. By selecting the correct combination of these parameters, the above phenomena can be isolated, identified, and/or corrected yielding valuable information about the sample's character.

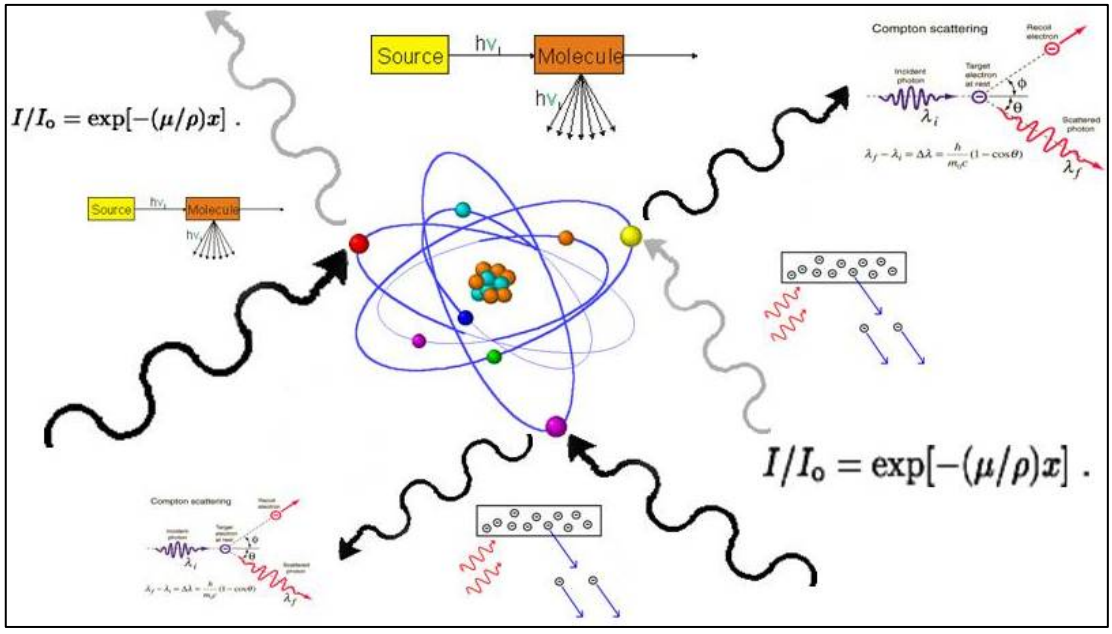

Figure 12: Abstract view of Physics involved in X-ray Spectroscopy

Interactions in the Detector

Sum Peaks

When two or more x rays enter the detector at the exact same time they are read and converted into one pulse with energy (e.g. amplitude) equal to the two pulses combined. Sum peaks appear on a spectrum when this occurs enough times to create a visible peak, as seen in Figure 13 and Figure 14. In theory, sum peaks can appear in any combination of characteristic energies, but they are most commonly found as double K_α-K_α, K_α-K_β and K_β-K_β because the higher rate of ocurrance of these x rays leads to a higher probability of a sum event being recorded. Although sum peaks are small, they may be mistaken as trace elements and cause spectral interference with other characteristic peaks.

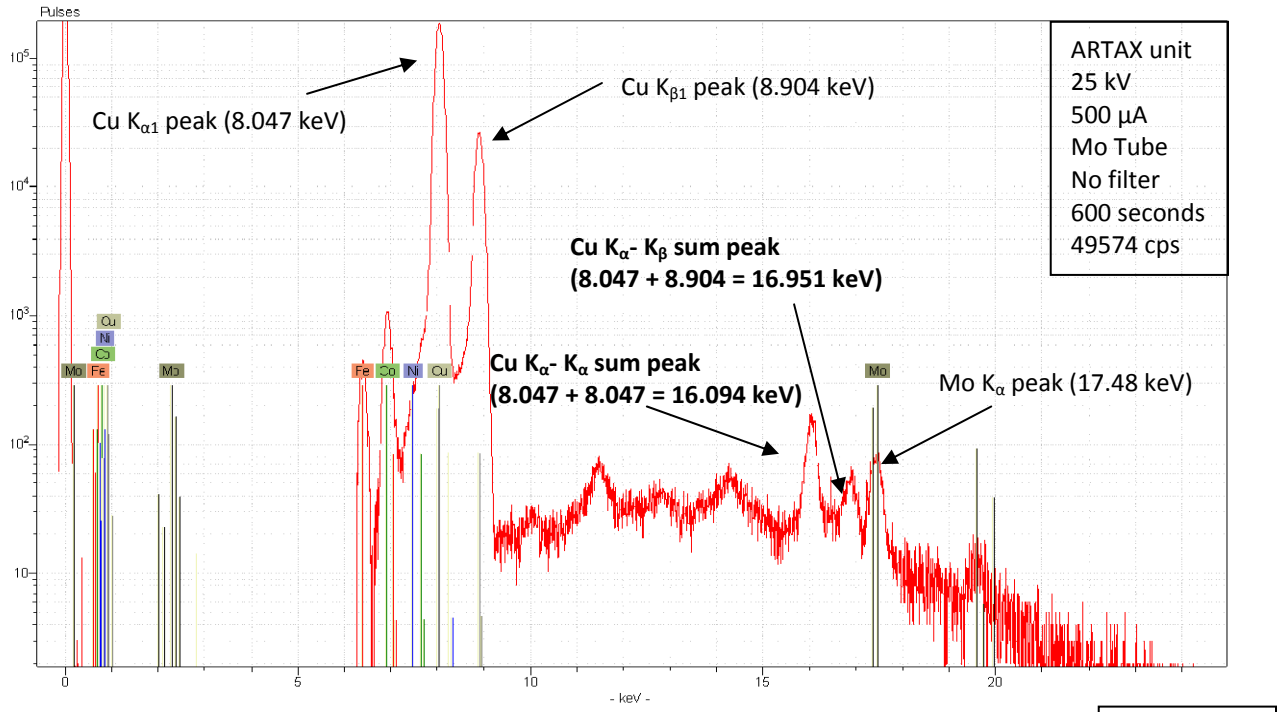

Figure 13: NIST standard C 1122 (see Appendix B for composition) spectrum on a logarithmic scale showing copper K_α and K_β peaks and their sum peaks

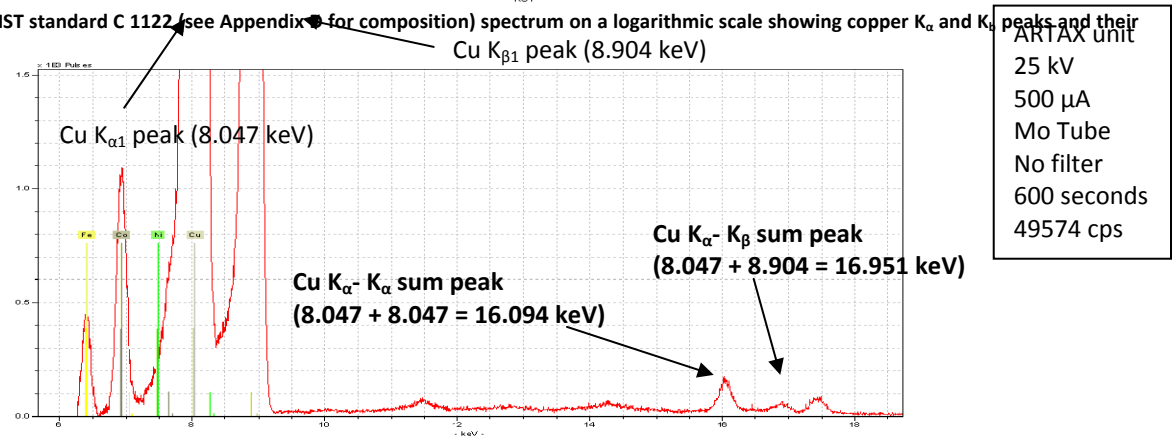

Figure 14: Linear scale of above spectrum

Escape Peaks

While most characteristic x-rays entering the detector are converted into pulses which are processed by the digital pulse processor, an incoming x-ray can excite and cause fluorescence in an atom in the detector. If the x-ray entering the detector has an energy greater than the absorption edge of an element in the detector (for the ARTAX and the TRACeR: Silicon), then fluorescence in the detector may occur. Figure 15 shows the typical relationship between incoming x ray energy and resulting Si escape peak counts. The inbound x ray will lose the amount of energy required to fluoresce the detector atom, leaving the x ray with an energy $E' = E_{inbound} - E_{Characteristic\ energy\ of\ detector}$, thus causing the detector to read the x ray as having an energy of E'.

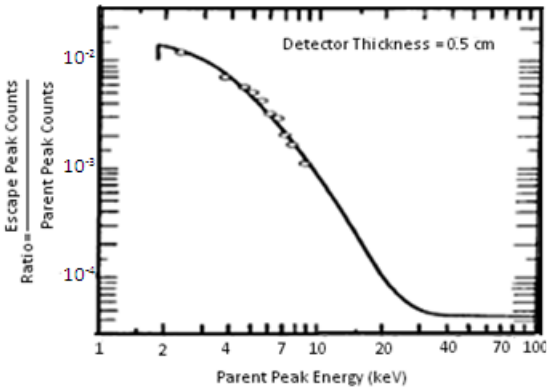

Figure 15: Typical relationship between escape peak count and parent energy peak. Parent peak energies closer to the absorption edge of silicon will create more escape counts

Escape peaks are much less intense than the characteristic peaks from which they are derived. Several escape peaks can occur in one spectrum, given that all characteristic energies above the absorption edge of the detector are capable of causing fluorescence. In the case of a Si based detector, escape peaks will appear approximately 1.74 keV lower than a characteristic peak because silicon has a K_α absorbtion edge. **Error! Reference source not found.** shows the escape peak from the Cu K_α peak. This figure also shows detector edge effect, which occurs at approximately 60% of the total K_α parent peak energy. Escape peaks can be automatically corrected by computer algorithms and software that calculates and outputs a corrected data curve (see Figure 17 and Figure 18).

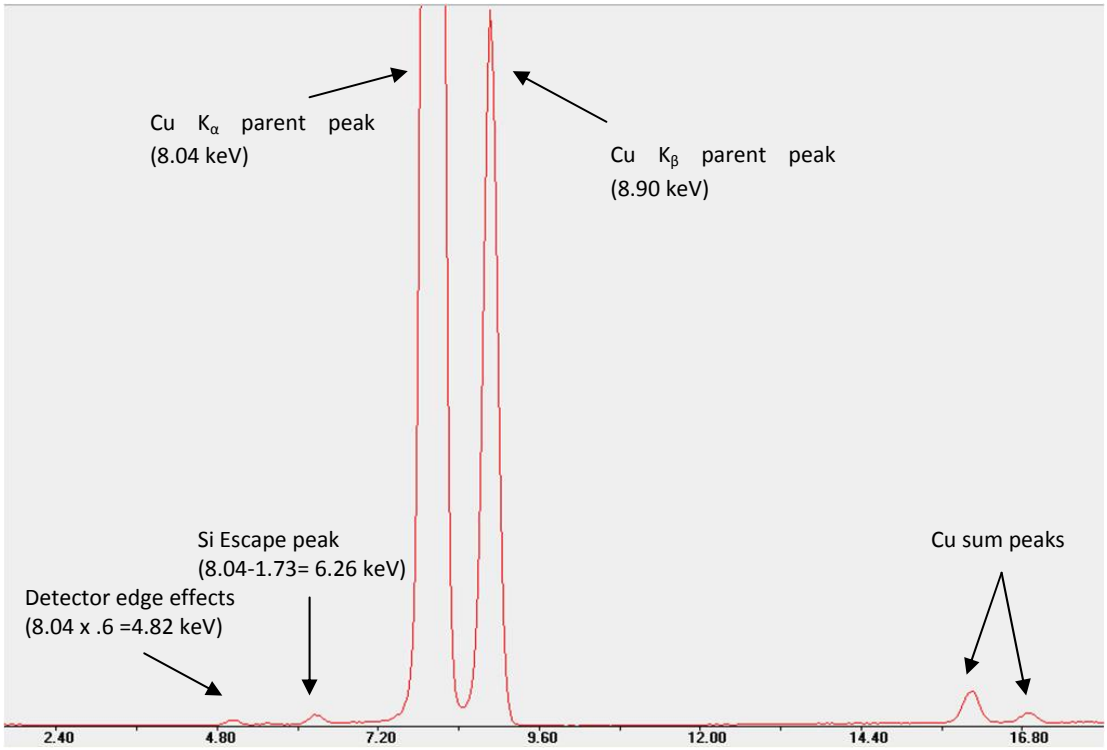

Figure 16: Spectra from a TRACeR model showing both the Si escape peak off of a Cu parent peak and the detector edge effects.

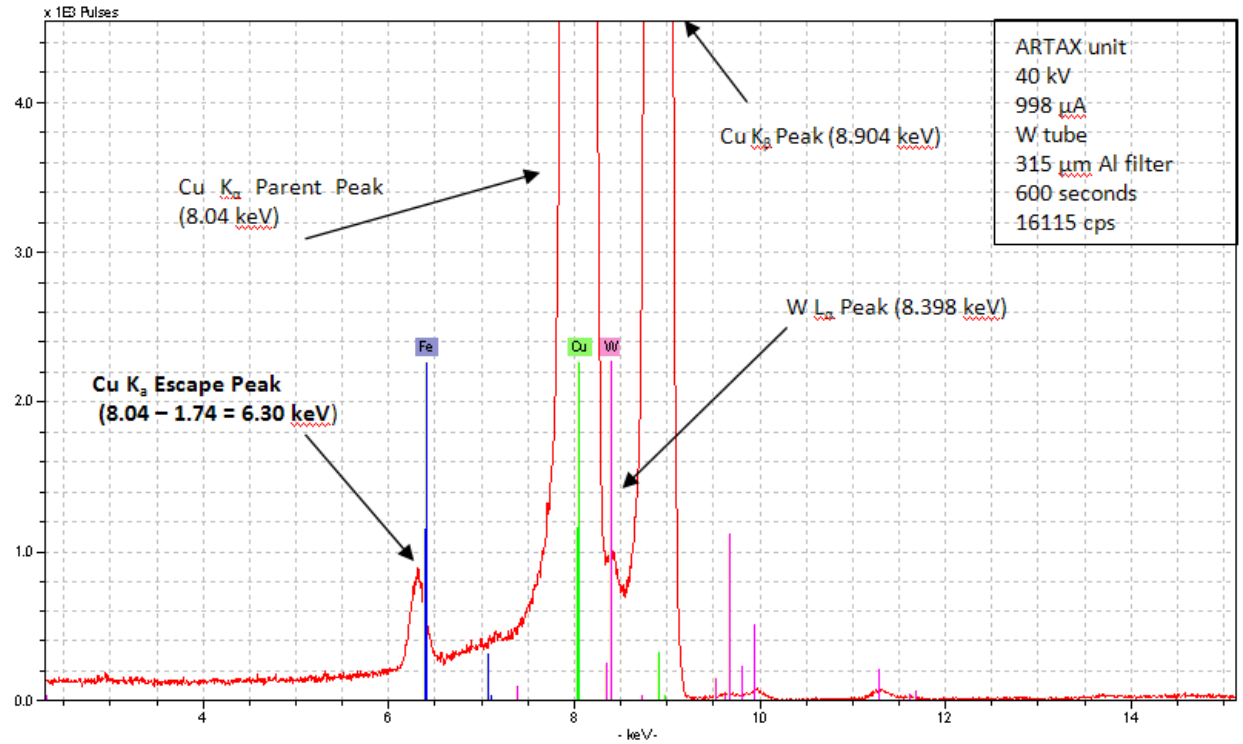

Figure 18: Linear scale spectrum of a NIST standard C 1122 (see Appendix D) without the corrected data curve shows the appearance of the Cu escape peak.

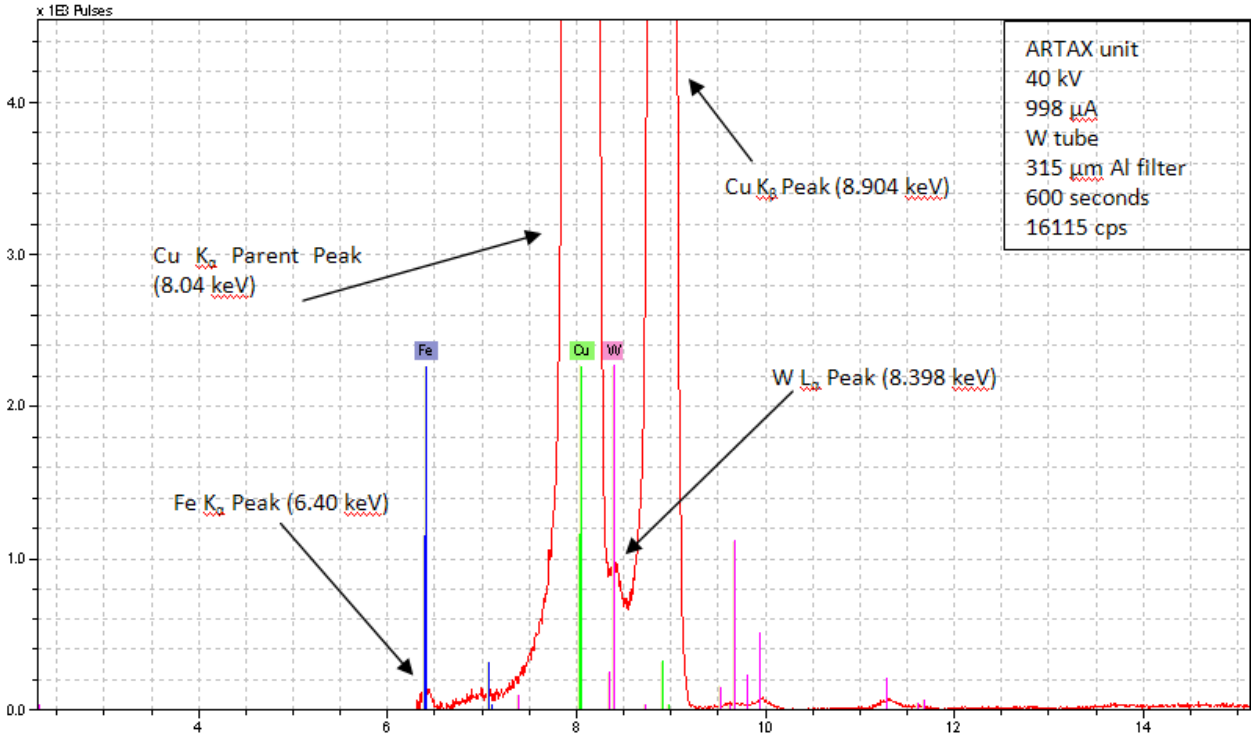

Figure 17: By applying the corrected data curve, the escape peak is removed and the true character of the sample is shown.

HETEROGENEITY

After radiation enters the detector and converts to pulses, discrepancies between peaks due to similar energy levels may occur. Heterogeneity can occur with any combination of lines, including different elements characteristic peaks, sum peaks, satellite peaks, escape peaks, etc. The resolution of the detector determines the amount of overlap between similar peaks.

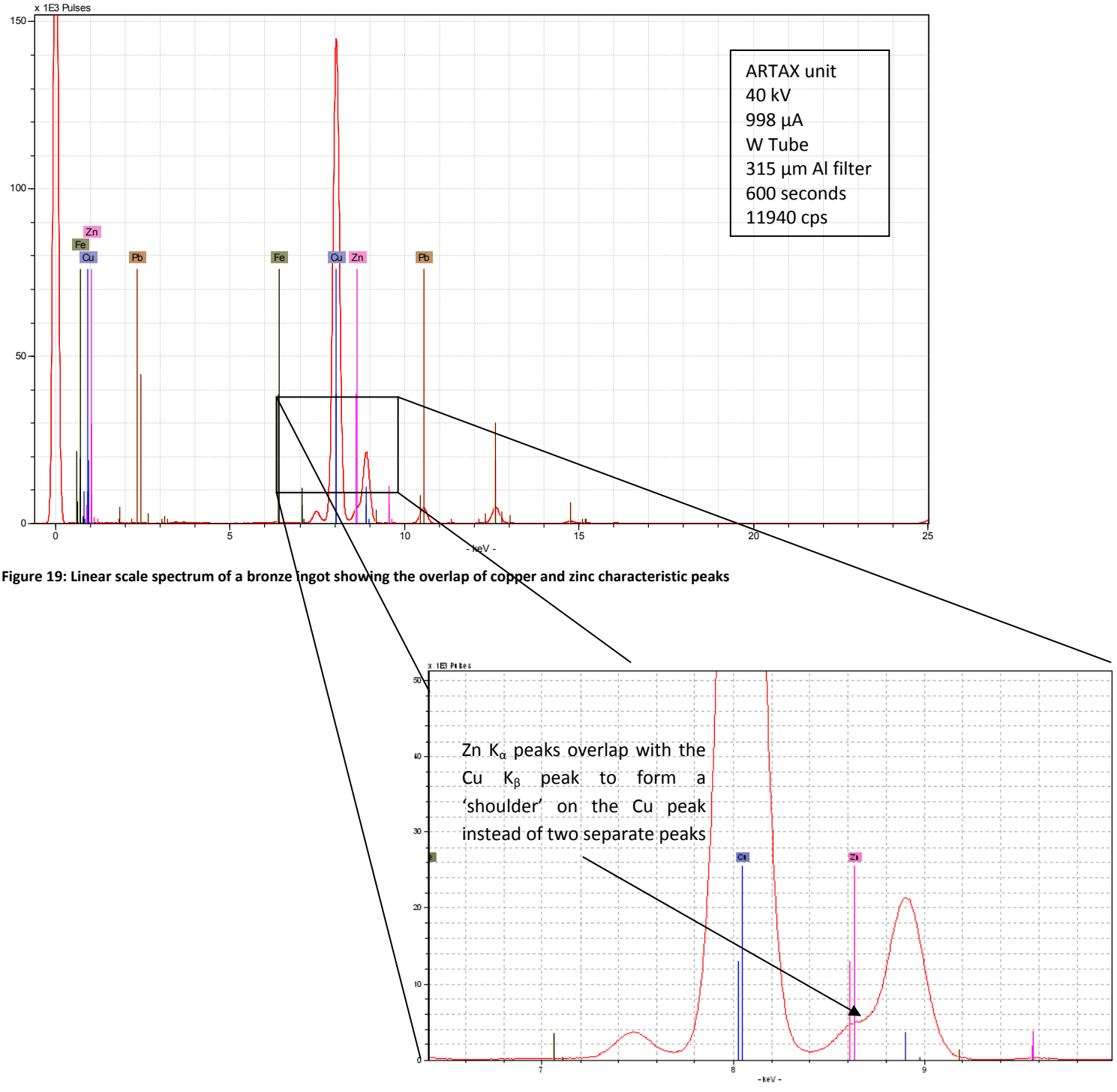

Figure 19: Linear scale spectrum of a bronze ingot showing the overlap of copper and zinc characteristic peaks

HETEROGENEITY (CONTINUED)

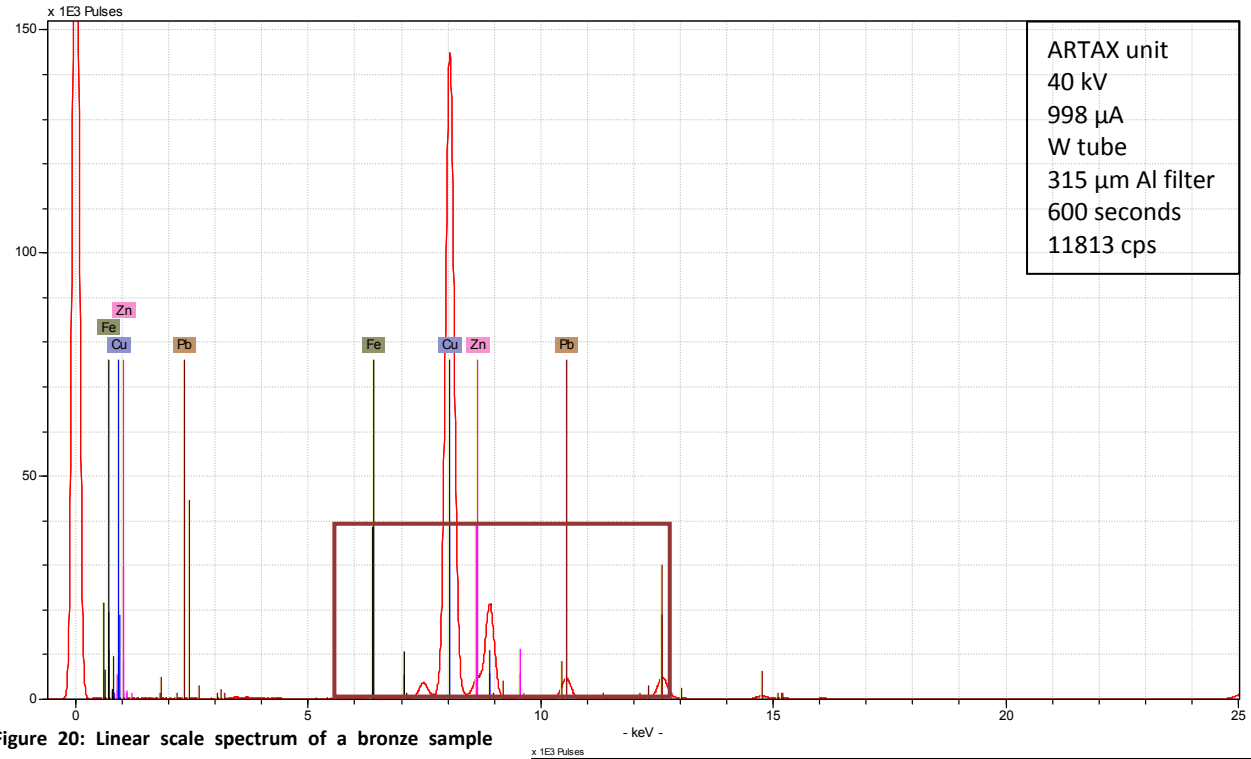

Figure 20: Linear scale spectrum of a bronze sample showing the effect of overlapping lines

The Si K_α escape peak off of the Cu K_α peak (6.31 keV) can be easily confused with the Iron K_α peak (6.40 keV). Figures 31-33 show the affect overlapping peaks can have on apparent sample character.

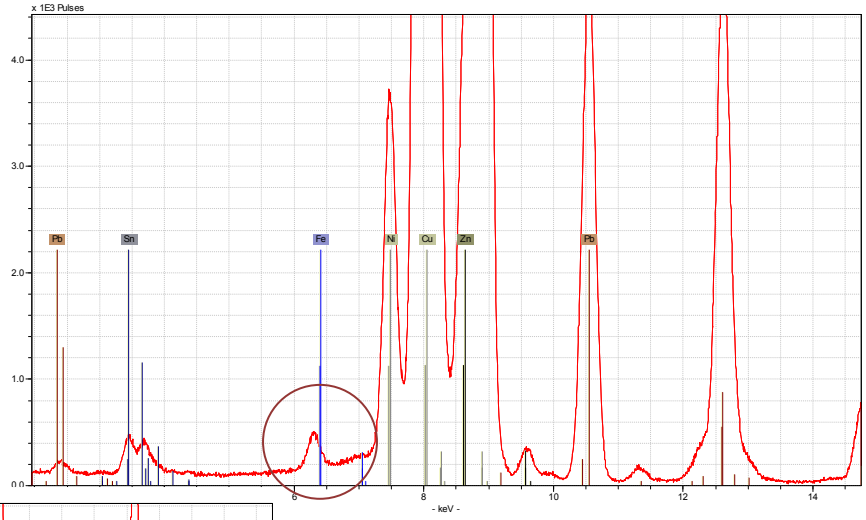

Figure 21: Close-up linear scale spectrum without the corrected data curve. The Cu escape peak appears to be a Fe peak

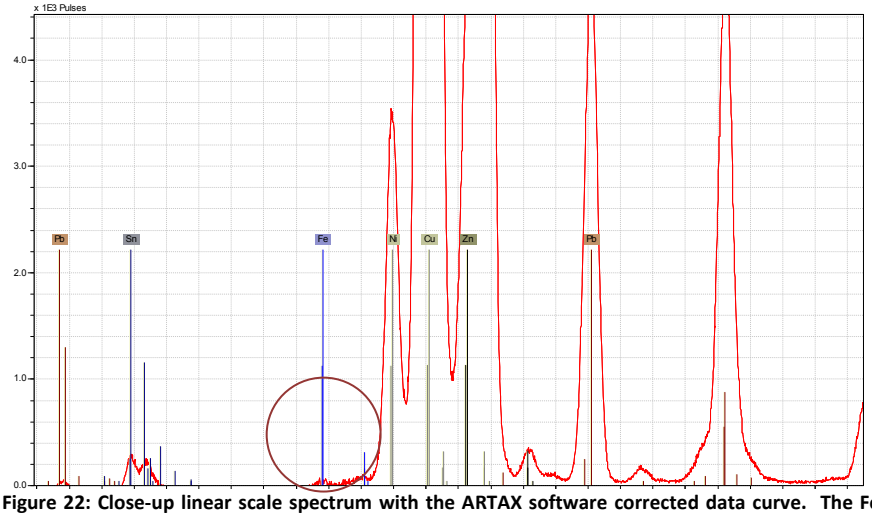

Figure 22: Close-up linear scale spectrum with the ARTAX software corrected data curve. The Fe peak is drastically lower than with the escape peak on top

The downside of using a corrected data curve is the possibility of removing or diminishing true sample lines.

Interference with Instrumentation

Equipment and Instrument Contribution

As the incident radiation travels from the source to the sample, it may cause fluorescence in materials in the machine which may be detected and shown on the spectrum. The target element may be detected (see Figure 23) in addition to iron, zinc, copper, and nickel in the tube, collimators, lens, etc (see Figure 24). By adding a filter in between the tube and the sample, much of this unwanted radiation can be removed from the spectrum (see Figure 26).

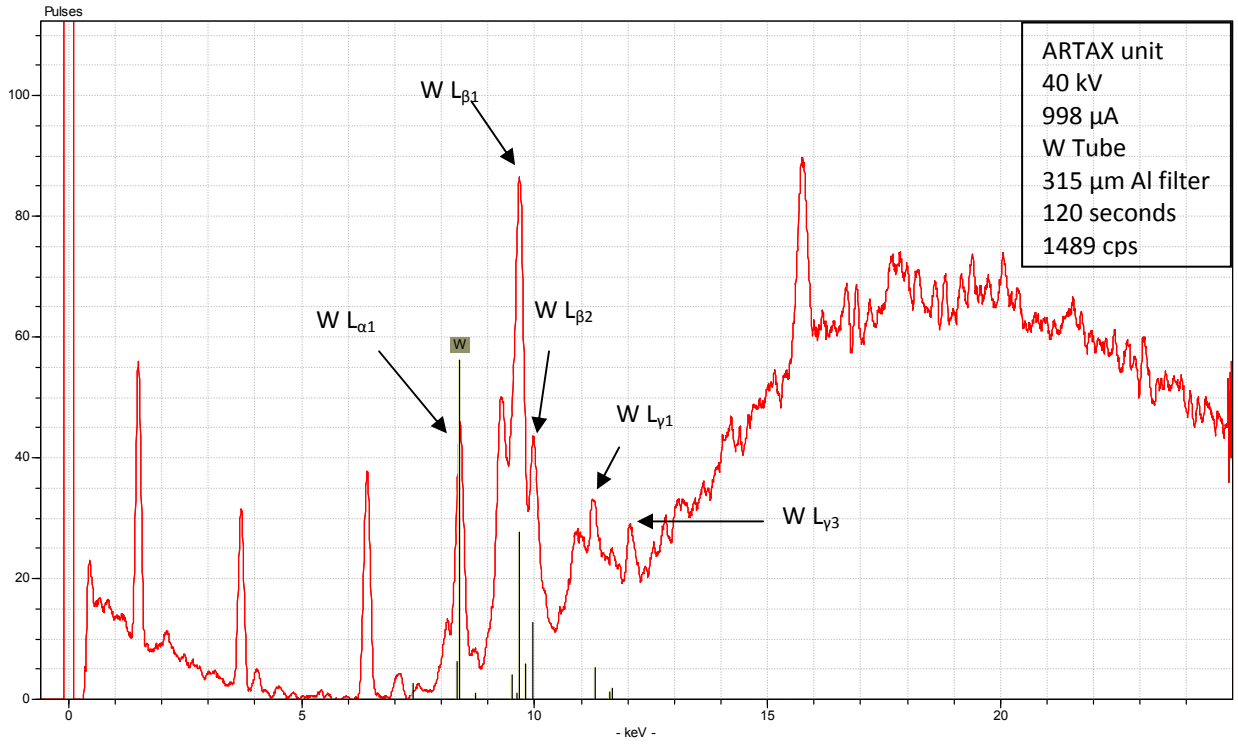

Figure 23: Linear scale spectrum of an Al_20_3 refractory with tungsten peaks from x-ray tube

Sources of Contribution

- X-ray tube target K and L lines (e.g. Cu, Rh, Mo, W, etc.)
- Stainless Steel Detector Can Lines (e.g. Fe, Co, Ni, only appear when testing low Z elements)
- Window lines (e.g. Ca)
- Collimator and instrument structure (e.g. Al)
- If using a thin film sample, elements in surface below the sample

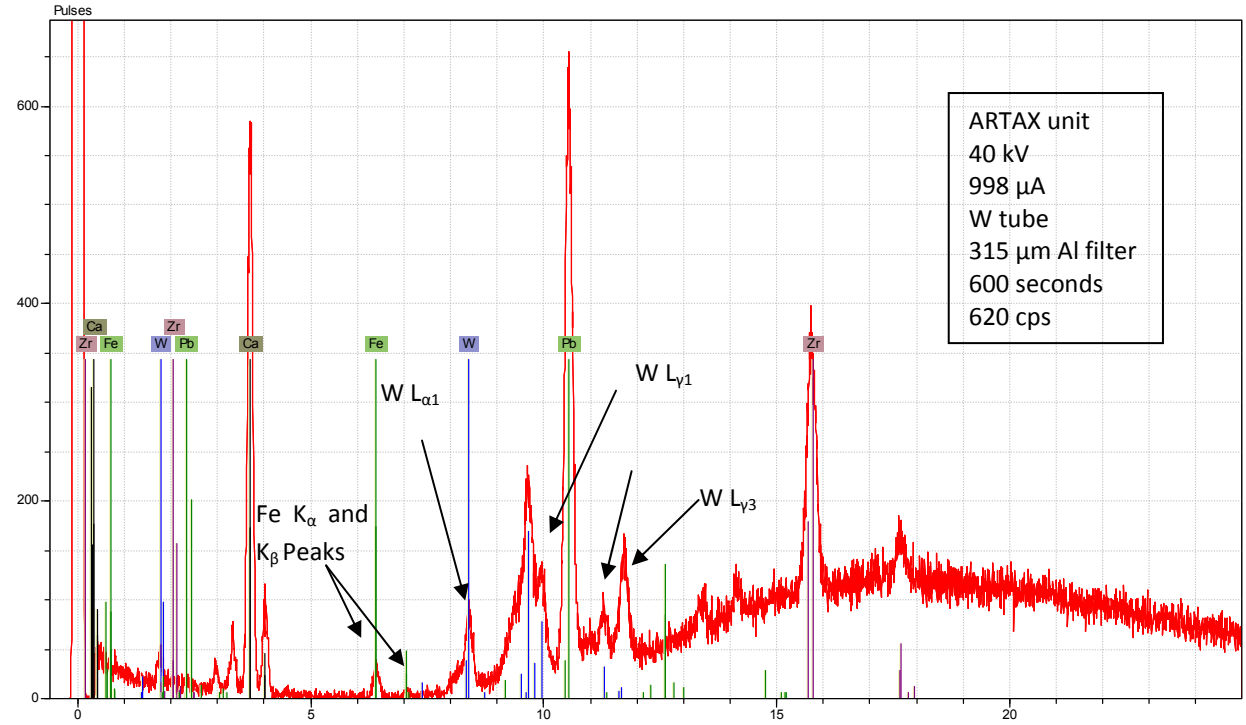

Figure 24: Linear scale spectrum of a Fe free microscope slide. Both W and Fe peaks appear on the spectrum because of ionization of the instrumentation

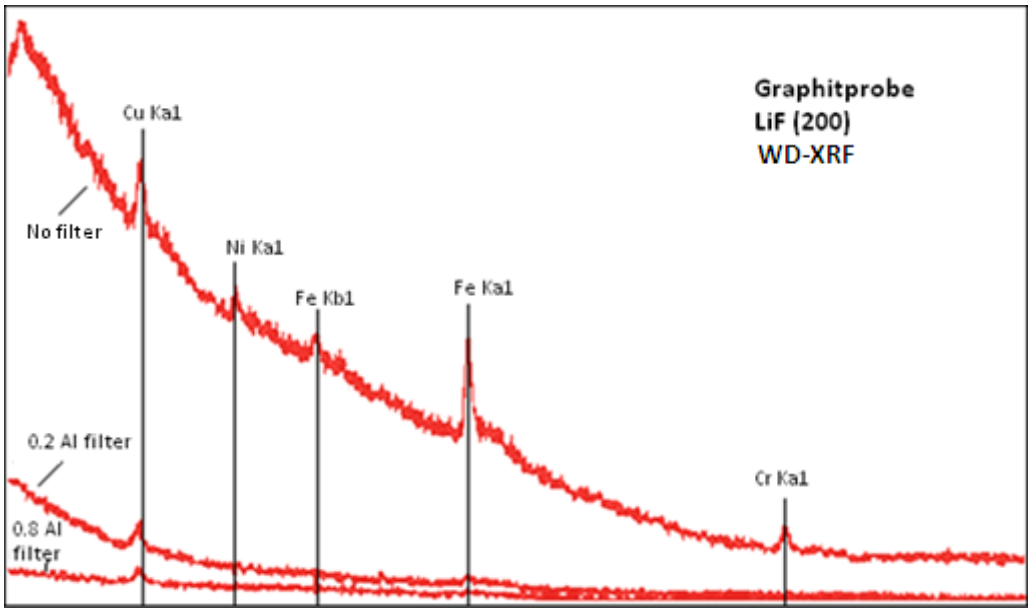

Figure 25: Linear scale spectrum showing the appearance of peaks of elements found in the can and other instrumentation (Ni, Fe, Cu, Cr). By adding a filter much of the unwanted radiation is removed from the spectrum. (Taken from Bruker AXS presentation "Introduction to X-ray Spectrometry")

THIN FILM ANALYSIS (BACKGROUND CONTRIBUTION)

X rays with high energy have the ability to partially penetrate through the surface of a sample. This phenomenon is also found in the use of filters, where a thin layer of metal or substance is used to attenuate certain energies from the exciting x ray beam that is incident on the sample of radiation. If the sample being tested is thin enough for the radiation to entirely penetrate through, elements in the surface below the sample may be fluoresced and detected. The figures below (see Figure 26, Figure 27, and **Error! Reference source not found.**) shows the effect of layering thin film samples and the detection of lower layers.

Figure 26: Measured separately, samples 1, 2, and 3 shows 11565, 21077, and 50522 counts of Pb, respectively. When the samples are layered in the order 3-2-1 the total counts increases to 55768 (around 5000 above that of just sample 3), indicating the partial detection of the lower layers of Pb. When the samples are layered 1-2-3 the total counts increases to 22757 (nearly 2x that of just sample 1), indicating the detection of lower layers is diminished but still affects the spectra

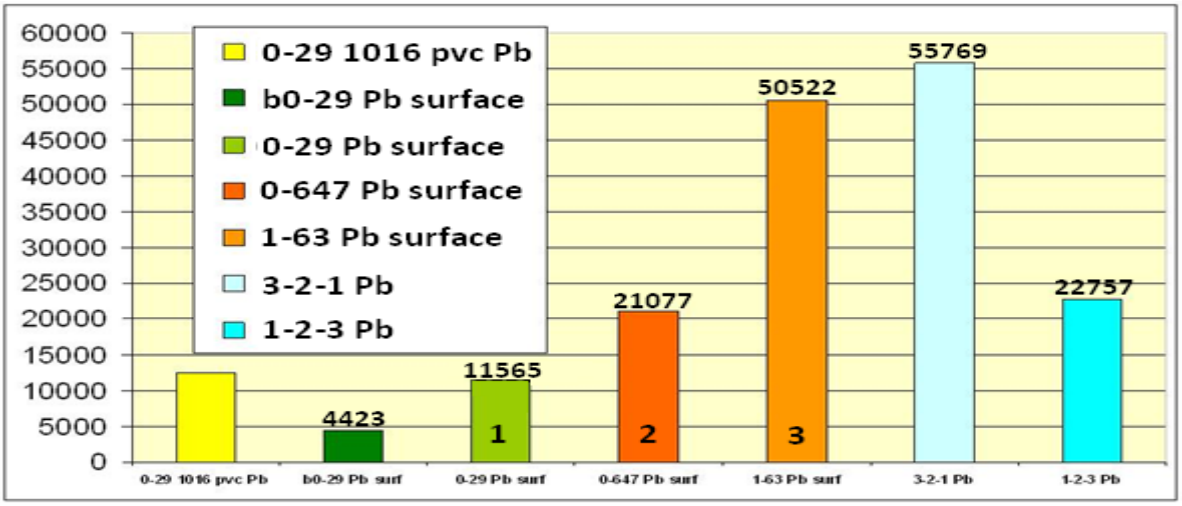

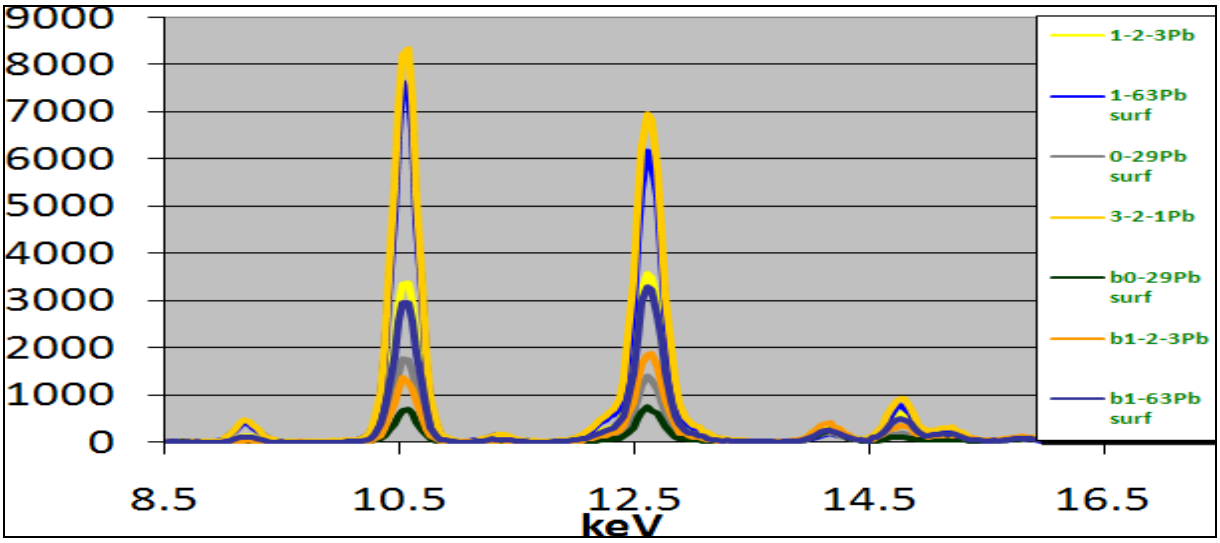

Figure 27: Spectra used in figure 26. Note the variation of the intensity shift of the Pb L alpha and Pb L beta depending where the highest concentration of Pb is in the sample. Highest close to the surface shows Pb L alpha about 15% more intense that Pb L beta. Lowest concentration close to the surface shows Pb L beta to be about 3% higher than Pb alpha.

PHENOMENA IN THE SAMPLE

RAYLEIGH (ELASTIC) SCATTERING

Incident radiation from the tube that reaches the sample is either absorbed in the photoelectric effect or reflected and scattered. When an x-ray reflects off the atoms of the sample without losing any energy it is called Rayleigh (or elastic) scattering. The energy of the outbound x ray will be equal to the energy of the inbound x ray, thus being detected as a source peak with the energy of the inbound x ray. The Rayleigh scatter peaks visible correspond with the characteristic energies of the x-ray tube target element. Figure 29 and Figure 30 show the appearance of Rayleigh peaks in a spectrum. Rayleigh scatter peaks are characterized by sharp shapes that are the same as the x ray flourescence peaks because they are produced in the detector by single energy x rays.

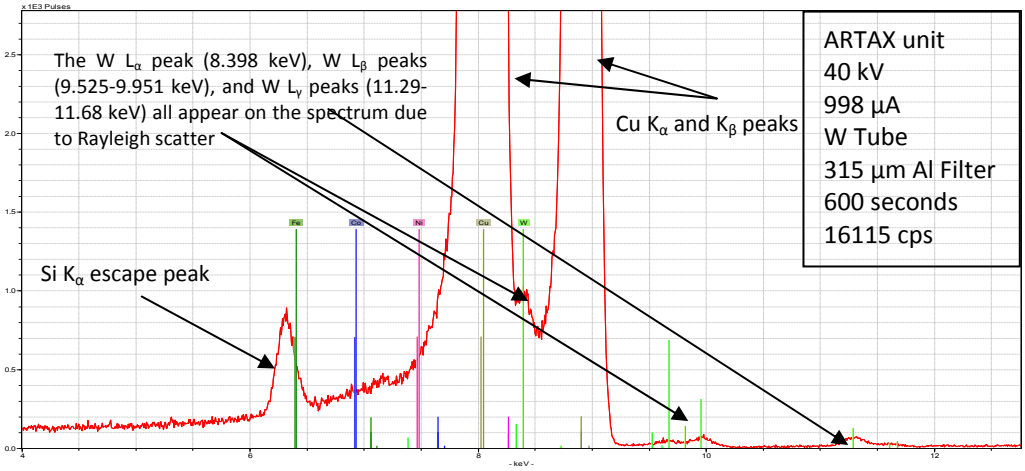

Figure 28: Close up linear scale spectrum of a NIST standard C 1251a (see Appendix D for composition) showing the appearance of the tungsten target Rayleigh scatter in spectra

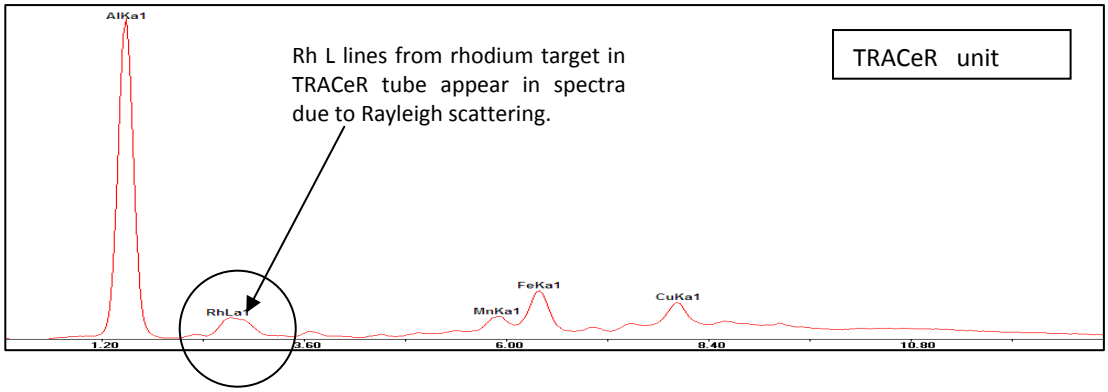

Figure 29: Close up linear scale spectrum showing the appearance of Rh characteristic lines in a spectrum due to Rayleigh scatter

RAYLEIGH (ELASTIC) SCATTERING (CONTINUED)

In addition to Rayleigh scatter peaks at the characteristic lines of the target in the tube, a Bremsstrahlung radiation curve may appear in the background of a spectrum due to Rayleigh and Compton scatter of all incident X-rays (Figure 31).

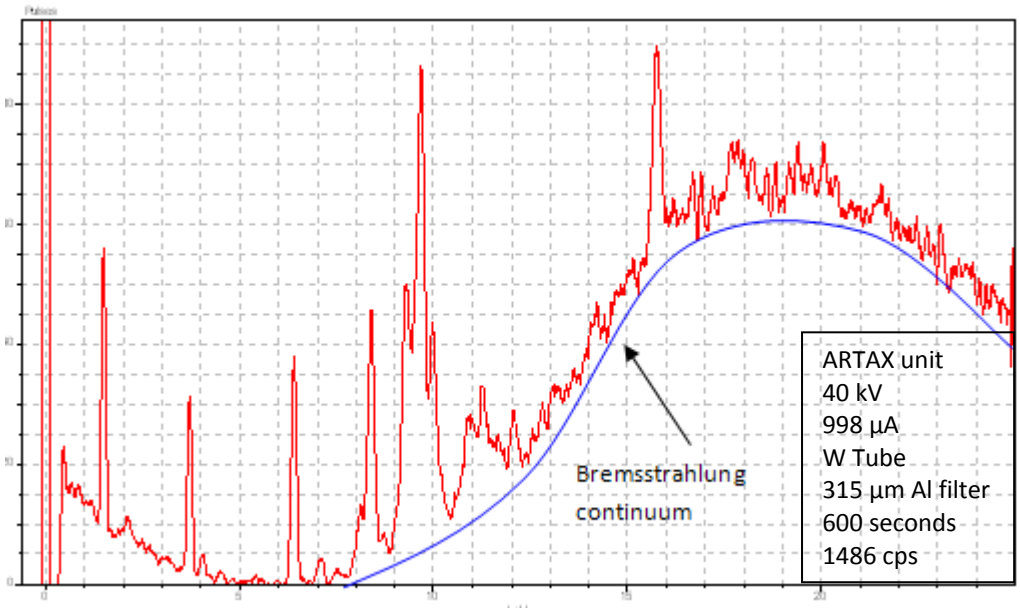

Figure 30: Linear scale spectrum of a high purity Al_2O_3 refractory with a well defined Bremsstrahlung continuum

COMPTON (INELASTIC) SCATTERING

Incident radiation with sufficient energy to ionize an inner-shell electron in an atom does not always cause fluorescence, but instead causes an excitation without losing all of its energy (see Figure 32). In these interactions, called Compton scattering, a x ray strikes an atom and loses energy, causing the excitement of an inner-shell electron. Because no vacancy is created in the atom, no characteristic energy is released; however, the x ray will lose energy and be scattered in all directions (noted by the formula in Figure 32). Compton scatter x-rays appear as a broad peak defined by the angle between the incident beam and the detector for the target characteristic x-ray lower in energy than Rayleigh scatter peaks because they only lose a small amount of energy in the excitation of an electron. They are generally broad due to the area of the detector and the area of the exciting beam, and they occur more often in low Z elements. Compton scattering can be seen in Figure 33.

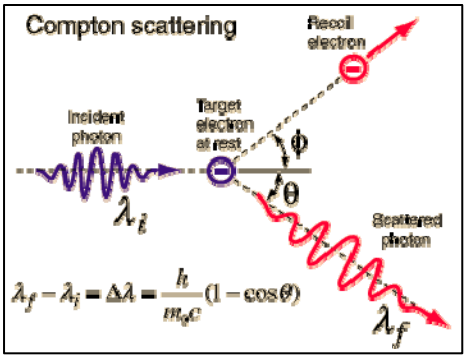

Figure 31: Compton scattering causes a shift in wavelength of the incident x ray

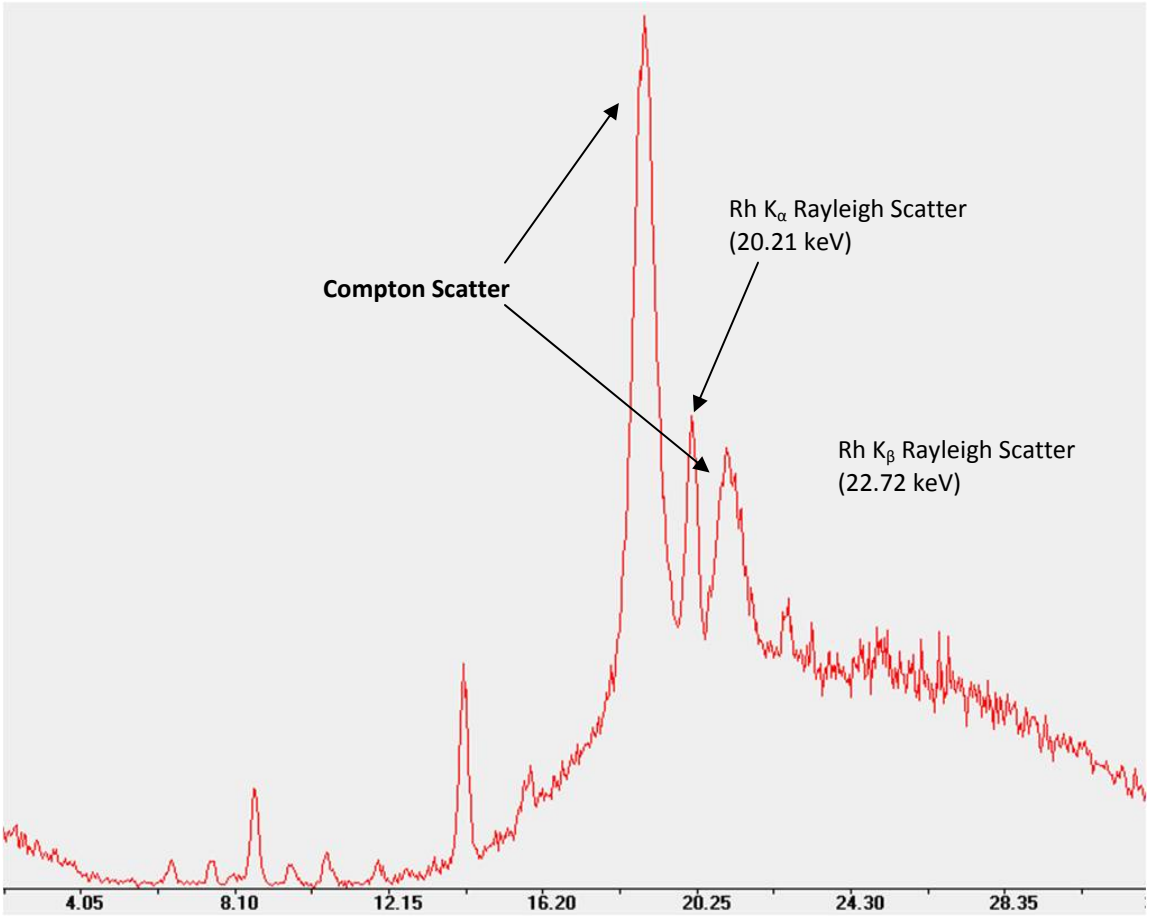

Figure 32: Linear scale spectrum showing Compton scattering of rhodium parent peaks on a TRACeR model.

MATRIX EFFECTS

Absorption: Any element that can absorb or scatter the incident x-rays is capable of reabsorbing characteristic x-rays of other elements (see Figure 34). After an atom undergoes the photoelectric effect and emits a characteristic x ray, the x ray may be reabsorbed by another atom in the sample. When this happens, it causes a misrepresentation of the counts of elements detected from the sample by failing to count a x ray for the initial element. The expected number of x ray counts recorded by the detector will be lower than expected because some are absorbed within the sample.

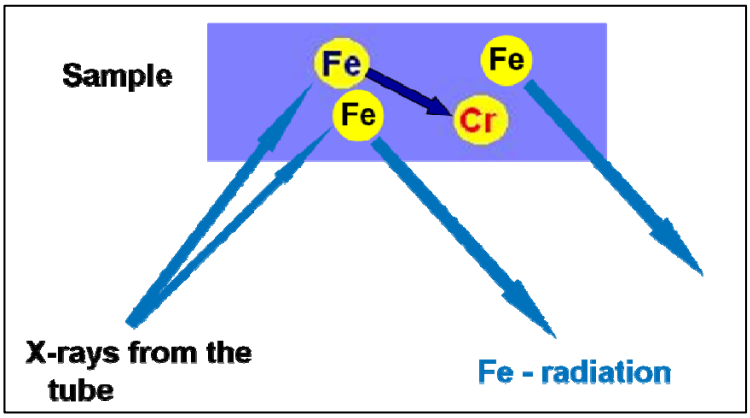

Figure 33: Example of secondary absorption.

Secondary Excitation: When the characteristic radiation from one atom is reabsorbed by another atom and has sufficient energy to ionize the atom, it will cause fluorescence in the second atom, producing only the characteristic radiation of the second atom (see Figure 35). This can lead to a misrepresentation of elements by enhancing the appearance of elements through secondary excitation.

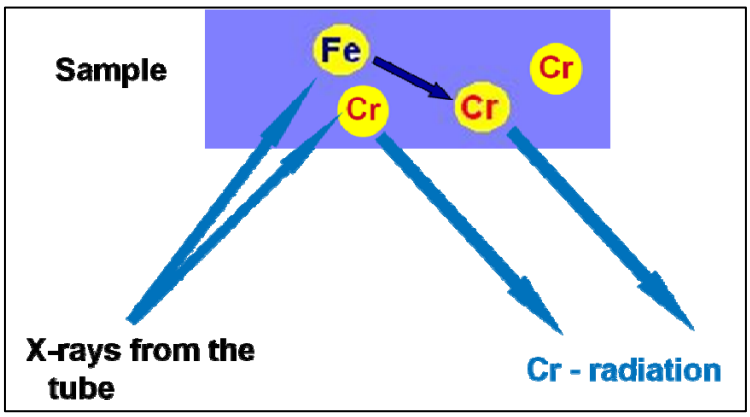

Figure 34: Example of secondary excitation

BRAGG SCATTERING

Many samples are composed of a periodic arrangement of atoms or molecules that create a crystal lattice. When a material exhibits a lattice structure, several different lattice planes can exist oriented in different directions. All planes that are parallel to a given lattice plane are a set distance away from one another, as established by the crystal structure.

When two parallel incident x-rays strike a pair of parallel lattice planes, the rays are reflected and can interfere with each other. This phenomenon is known as *Bragg scattering*, or the scattering of incident x-rays due to the crystal lattice of a sample. Bragg's law states that two waves interfere constructively when $n\lambda=2d\sin\emptyset$ where: n is the reflection order, λ is the wavelength of the incident x-ray, d is the distance between the lattice planes, and Ø is the angle of reflection upon the crystal lattice. According to Bragg's law, a given angle has a specific set of wavelengths (or energies) that can cause constructive interference. Samples with uniform crystal structure will exhibit narrow peaks, while a sample with a non uniform crystal lattice will be broader. All the data used in the examples below are taken with the Artax system. The sharper lines in Figure 37 suggest that the sample is of higher quality (more uniform crystal) than that in Figure 38.

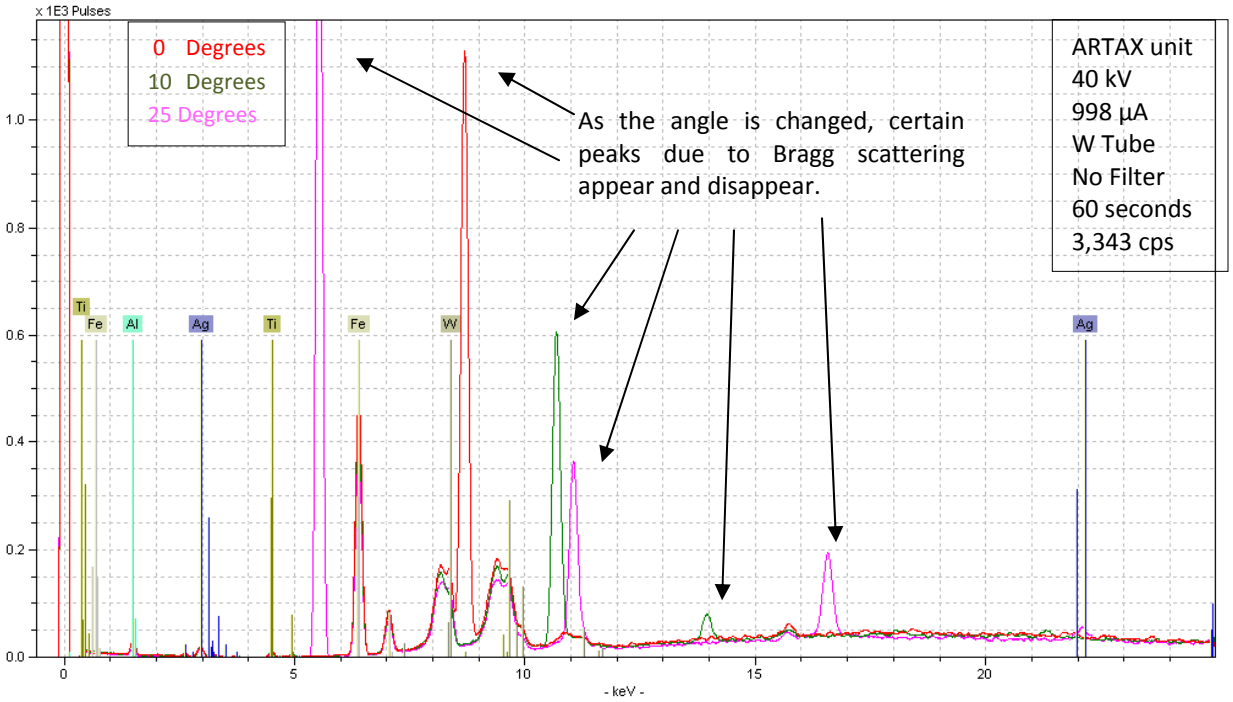

Figure 35: Linear scale spectrum of a blue gemstone showing the effect of incident angle on Bragg peaks

If the sample has a preferred crystal orientation, only a small angle is required for Bragg scattering (<1°), so Bragg scattering can be identified and prevented by changing the angle of incidence of the x-ray to the sample. In doing so, a peak in one graph will not appear on another because the angle that satisfies Bragg's law has been changed. To ensure that Bragg peaks are not confused with characteristic lines of elements, the angle of incidence between the incident x-ray beam and the sample can be altered, thus disconnecting the constructive interference which creates Bragg peaks.

When the sample does not have a strongly preferred crystalline orientation as in the case of a gemstone, by adding a filter it is possible to eliminate Bragg peaks by removing the specific wavelengths that create constructive interference. However, sometimes Bragg peaks are impossible to remove without interfering with the region of interest.

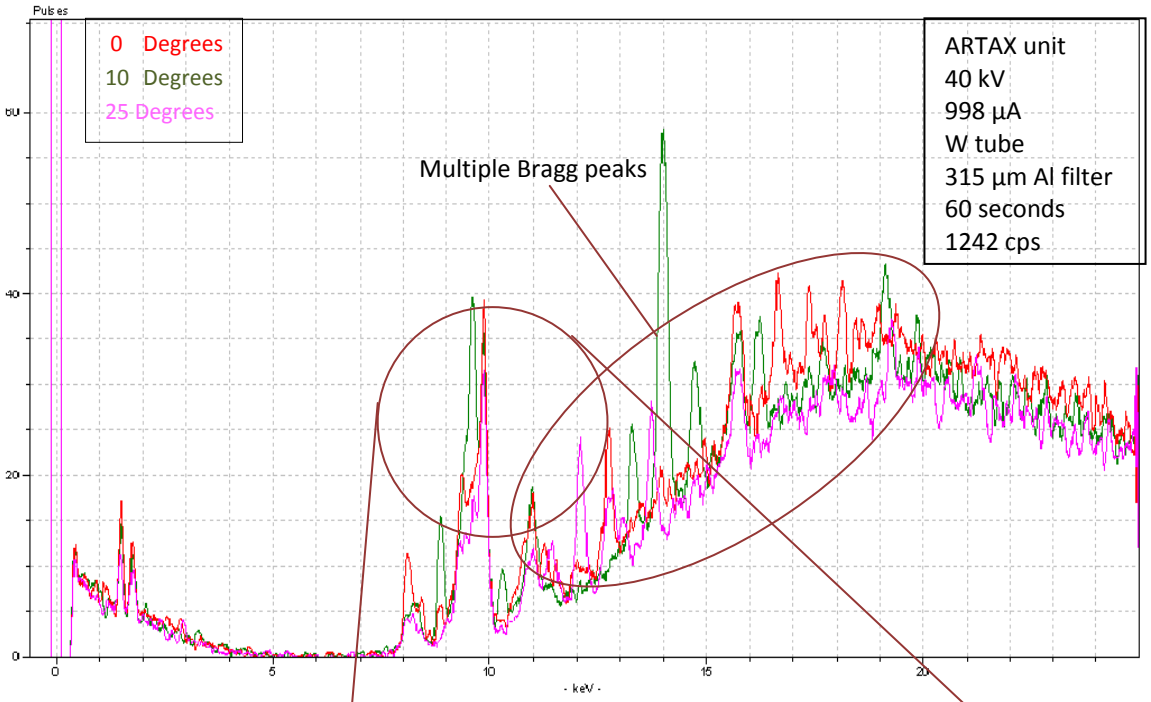

Figure 36: Linear scale spectrum of a green gemstone at angles 0, 10, and 25, showing the changes in Bragg peaks and their effect on other characteristic peaks.

Bragg Scattering can interfere with peaks and cause a misrepresentation of elements in the sample. In this example, the peak is greatly enhanced by Bragg scattering in the green spectrum, whereas the pink spectrum peak is not exaggerated because the angle was changed.

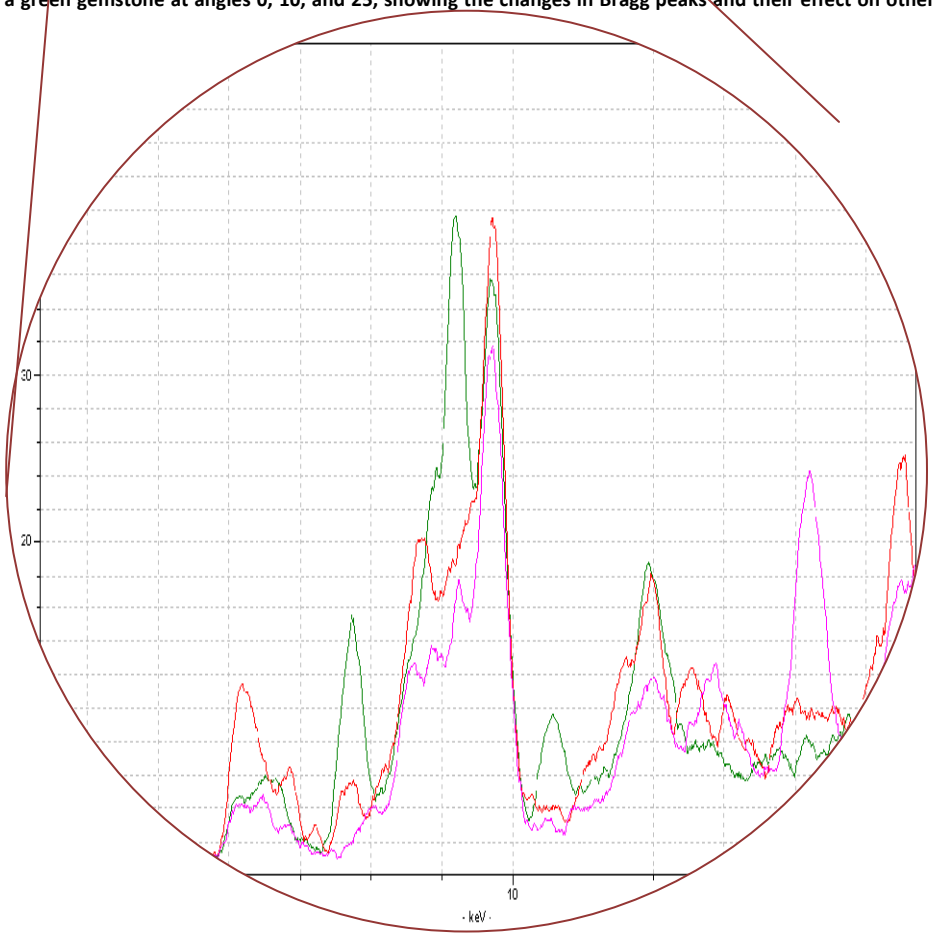

BRAGG SCATTERING (NIST C 1122 EXAMPLES)

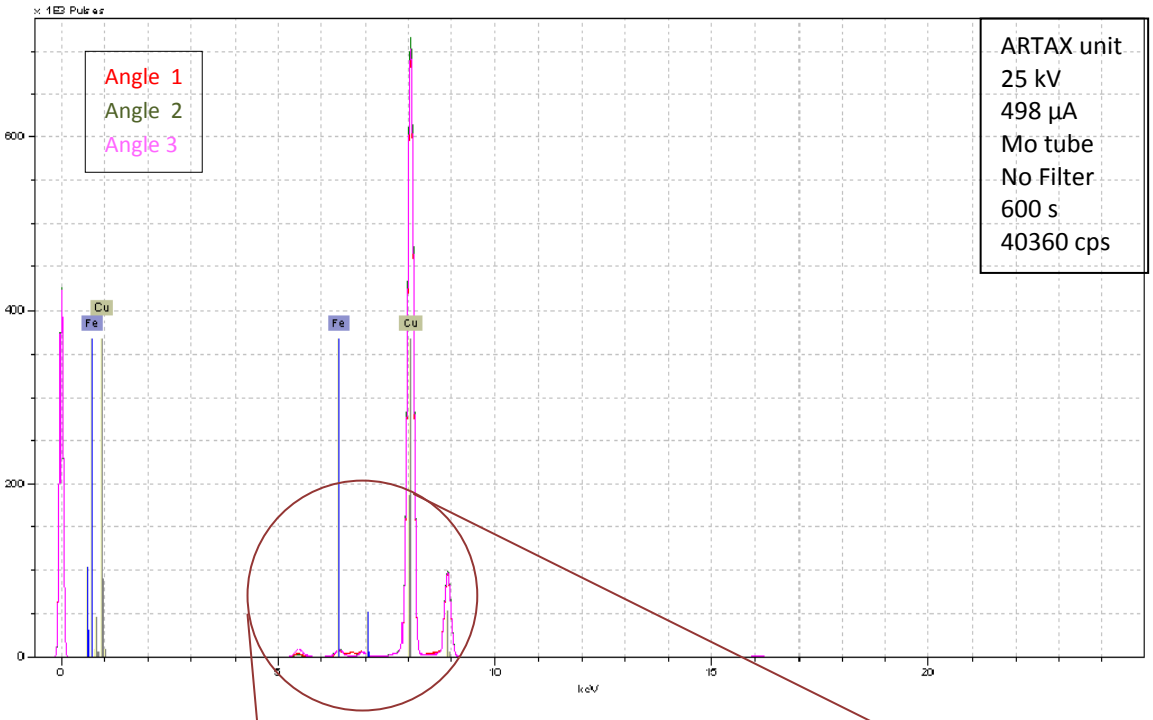

Figure 37: Linear scale spectrum of a NIST standard C 1122 (see Appendix D) sample with no filter exhibiting the Bragg peaks

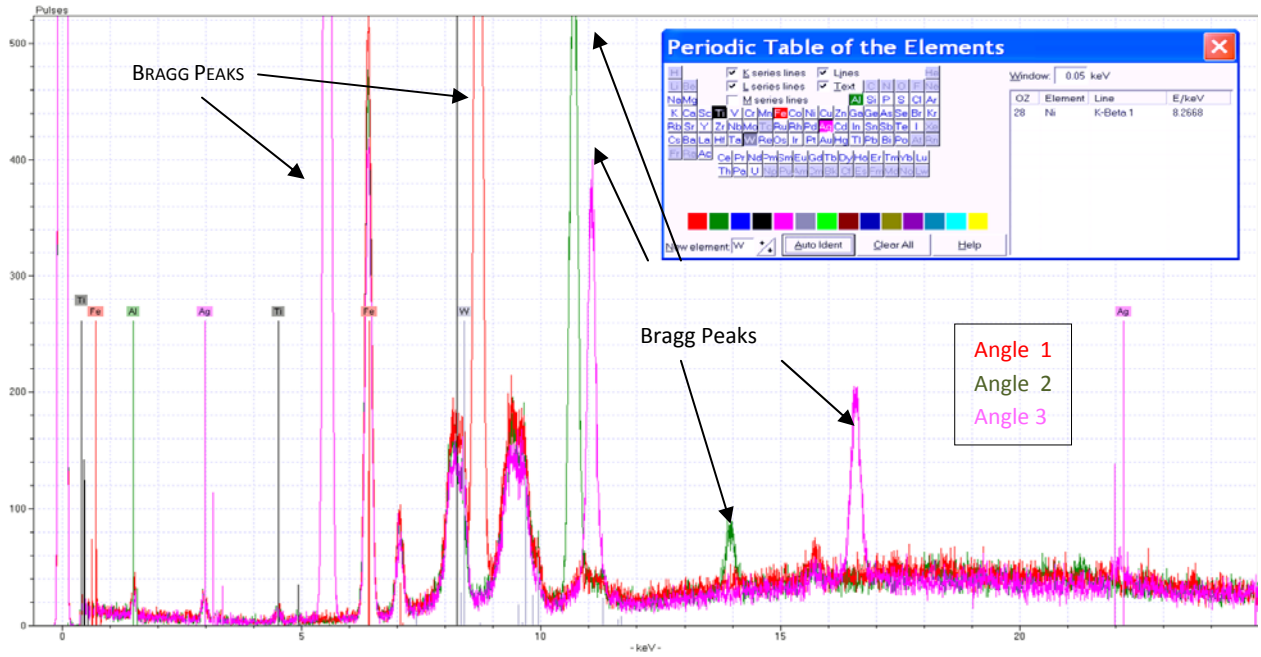

Figure 38: Bragg peaks appear in different intensities and positions based on the crystal orientation of the sample.

Bragg Scattering (Gemstone examples)

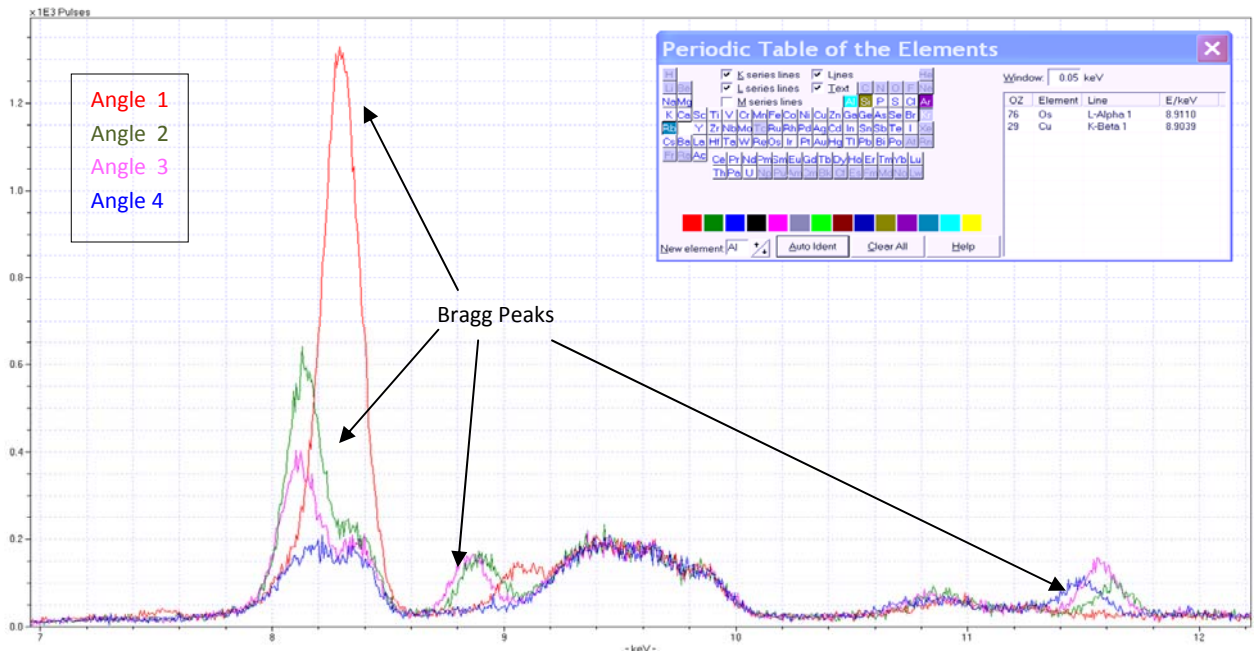

Figure 39: Certain Bragg peaks are amplified at specific angles, while diminished at others.

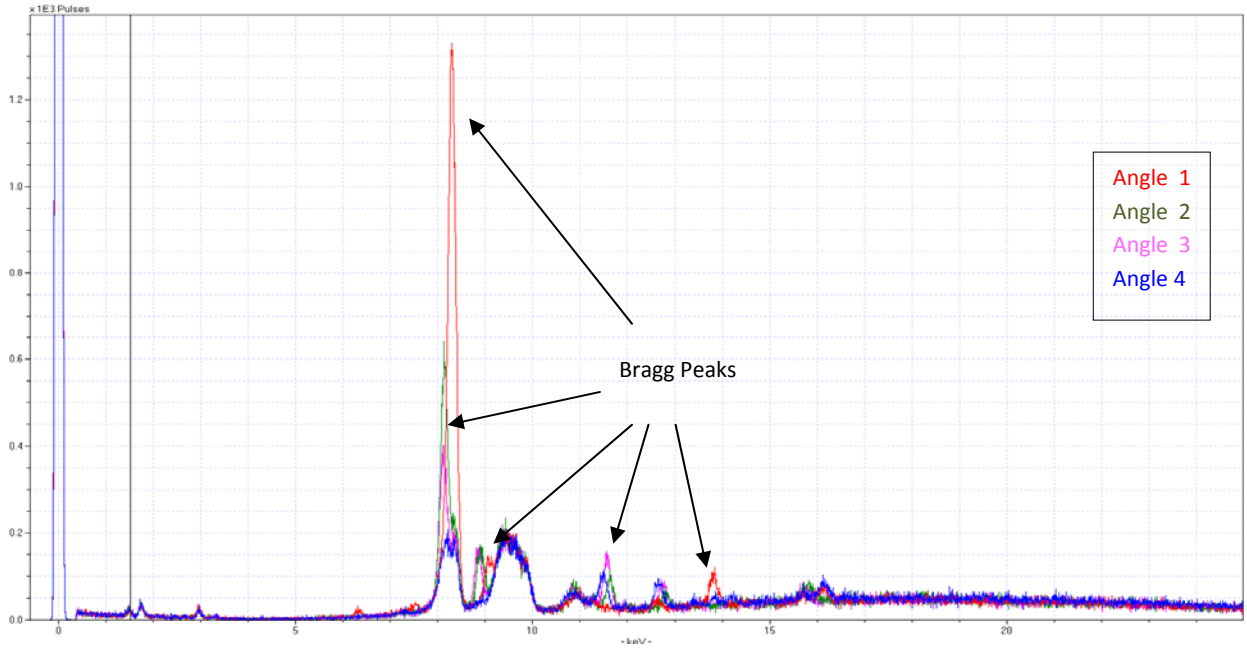

Figure 40: Bragg peaks may appear on top of other peaks, as seen in the red.

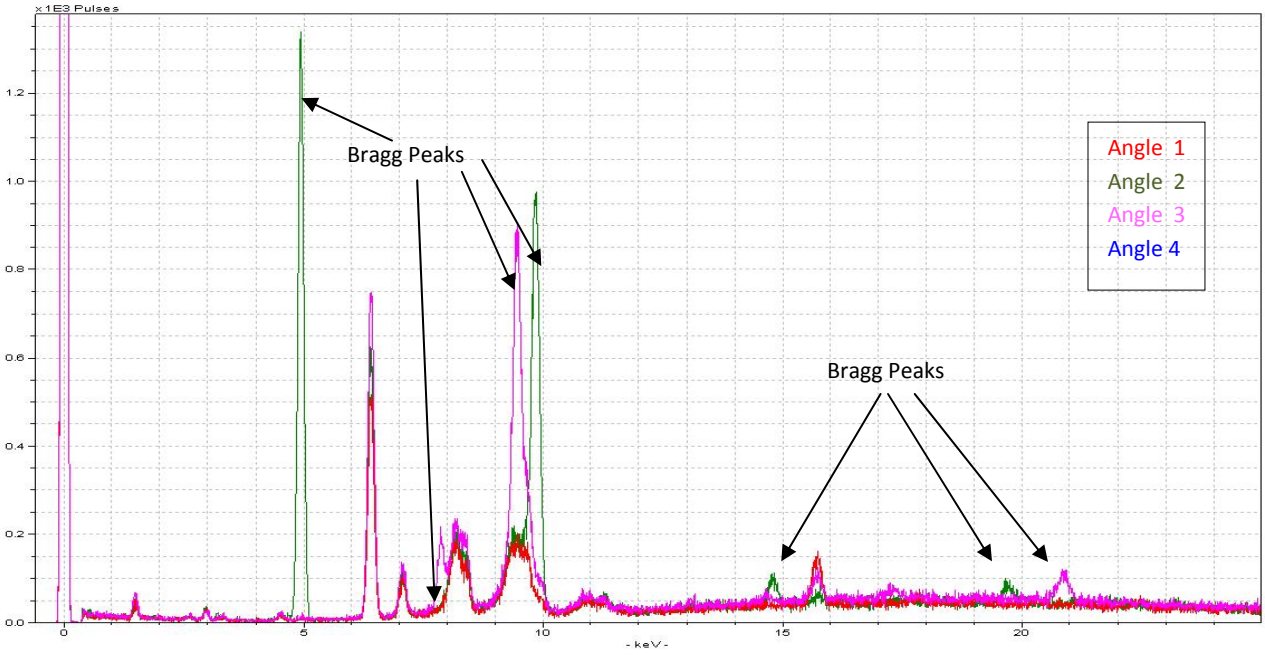

Figure 41: The red spectrum displays no Bragg peaks, while the green and pink have several different peaks

Field Applications

Identifying Genuine Artifacts (Chelsea Bullfinch Example)

With the increased portability and ease of use in the TRACeR and ARTAX units, several applications can be made in several different areas of study. The following are a few examples taken from a presentation by Dr. Bruce Kaiser on ED-XRF applications.

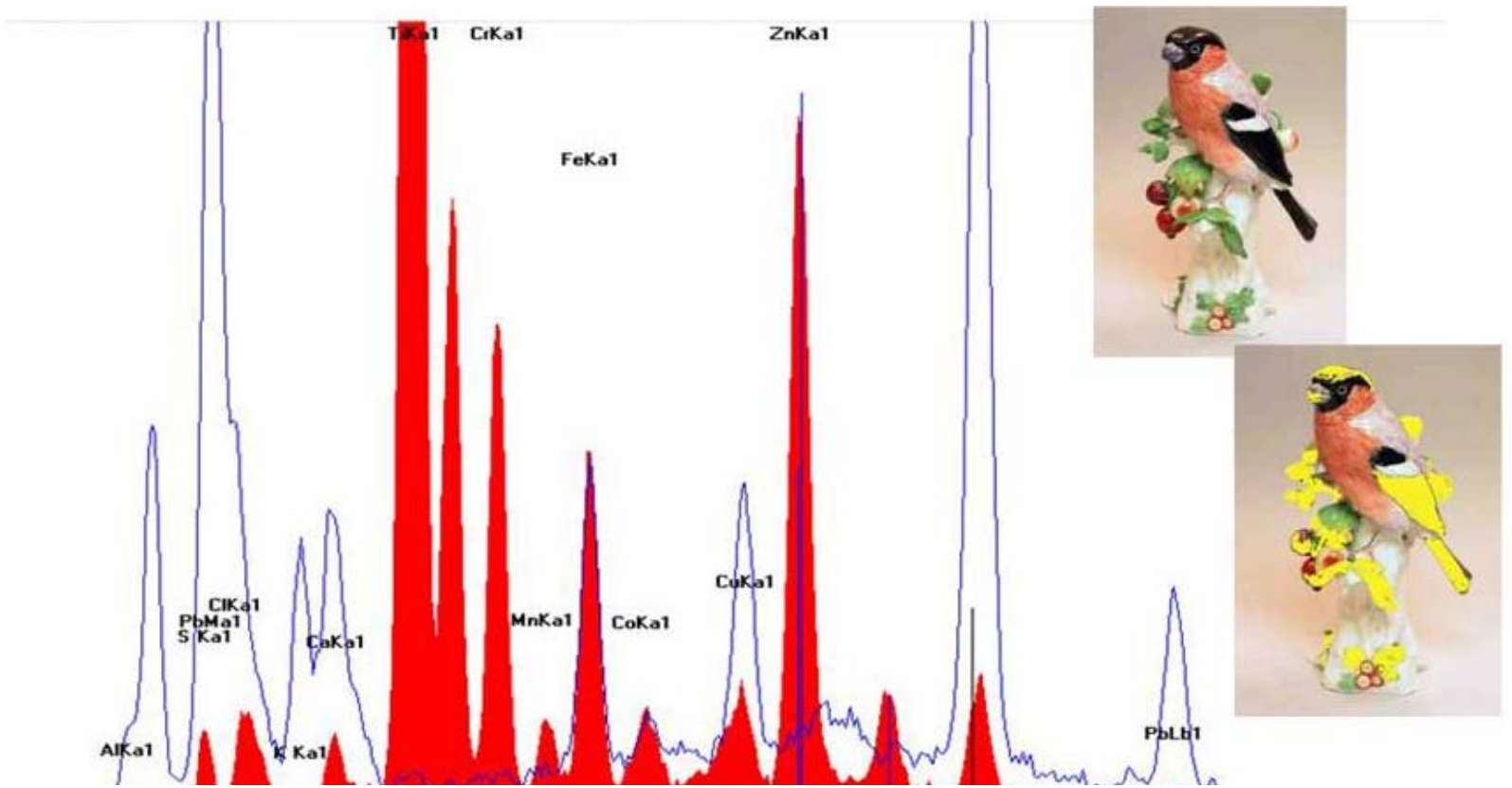

Figure 42: Overlapping spectra of the two different paints prove that the ceramic Bullfinch was restored from its natural condition.

IDENTIFYING TRUE ORIGINS (STONEWARE EXAMPLE)

By Using the TRACeR and XRF spectroscopy technology, historians can easily identify the origins of otherwise unknown artifacts. Here, English stoneware (blue spectrum) contains significantly more iron than German stoneware (red spectrum). By using this knowledge, historians can identify two visually identical pots.

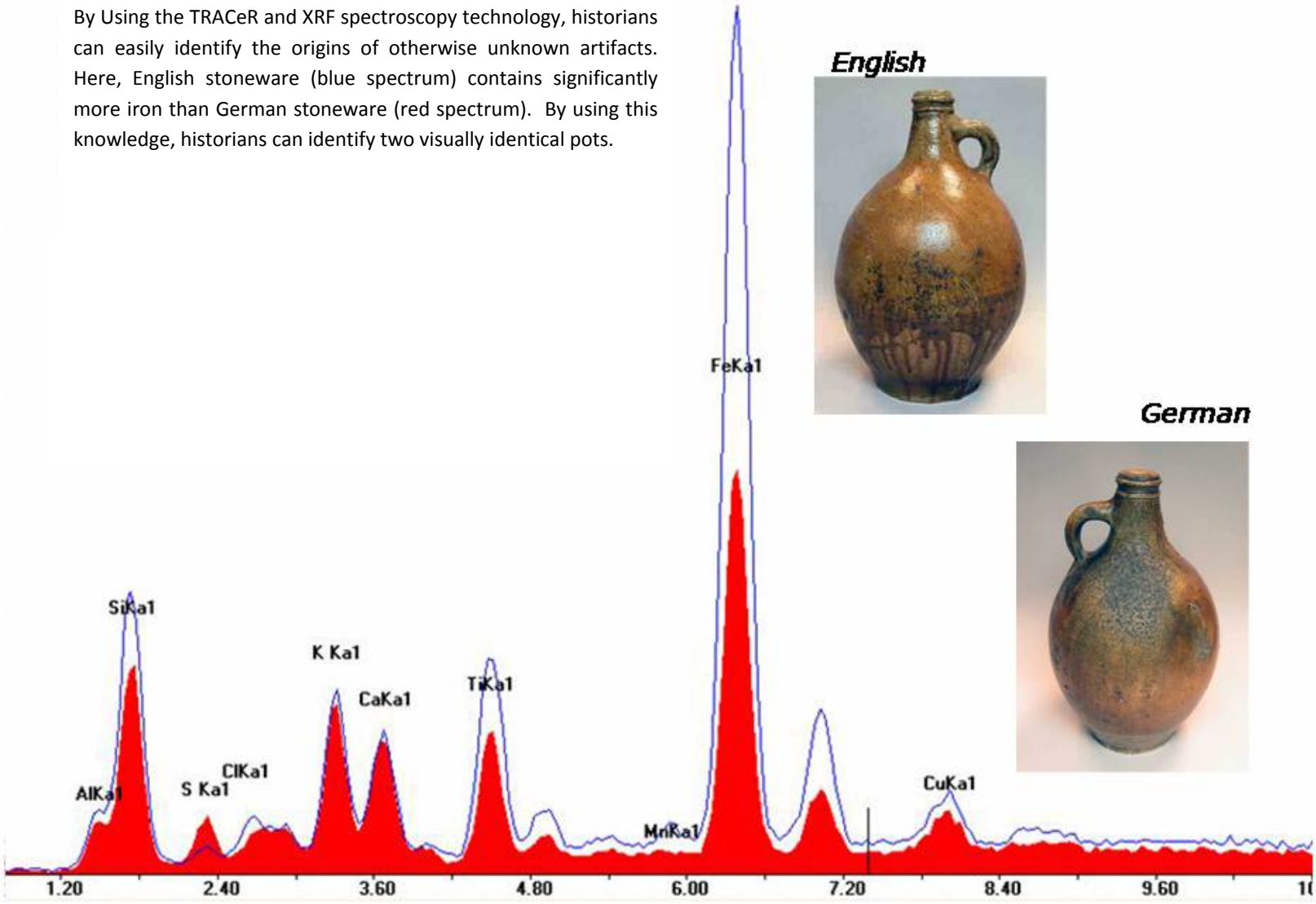

Figure 43: True origins of artifacts can be found using elemental analysis through XRF technology

Measuring Chlorine with the Tracer

Measurement of Cl is very important as it is often involved in corrosion and degradation of artifacts in marine environments. Or in some cases is a key constituent of pigments or other coatings, or an issue in paper conservation.

The following slides first depict how to make up thin film standards to determine the Cl surface content in micro grams per square centimeter. And then how to set the Bruker handheld xrf instrument up to measure levels as low as 10 micro grams per square and shows 2 applications.

It should be noted the Cl analysis is very much a SURFACE ANALYSIS when using xrf, as the Cl atom emits only a 2.7 keV x ray. This low an energy x ray is not able to escape the sample unless the atom is very near the surface.

Creation of very very thin film Chlorine Standards

- 1.83 gms of Zirconium dichloride oxide (ZrOCL2.8H2O) was added to 100 ml of distilled water.
- Then various amounts were pipetted on to light weight paper circles 8.2 cm in diameter
- The paper was saturated with the solution in each case to assure that the solution distributed uniformly over the entire surface
- Each paper was then let dry on a plastic sheet for 1 hour
- The resulting microgram/cm values for Zr and Cl

Zr-ug/sq-cm	Cl-ug/sq-cm
0.000	0.000
1.269	0.987
6.347	4.933
12.693	9.866

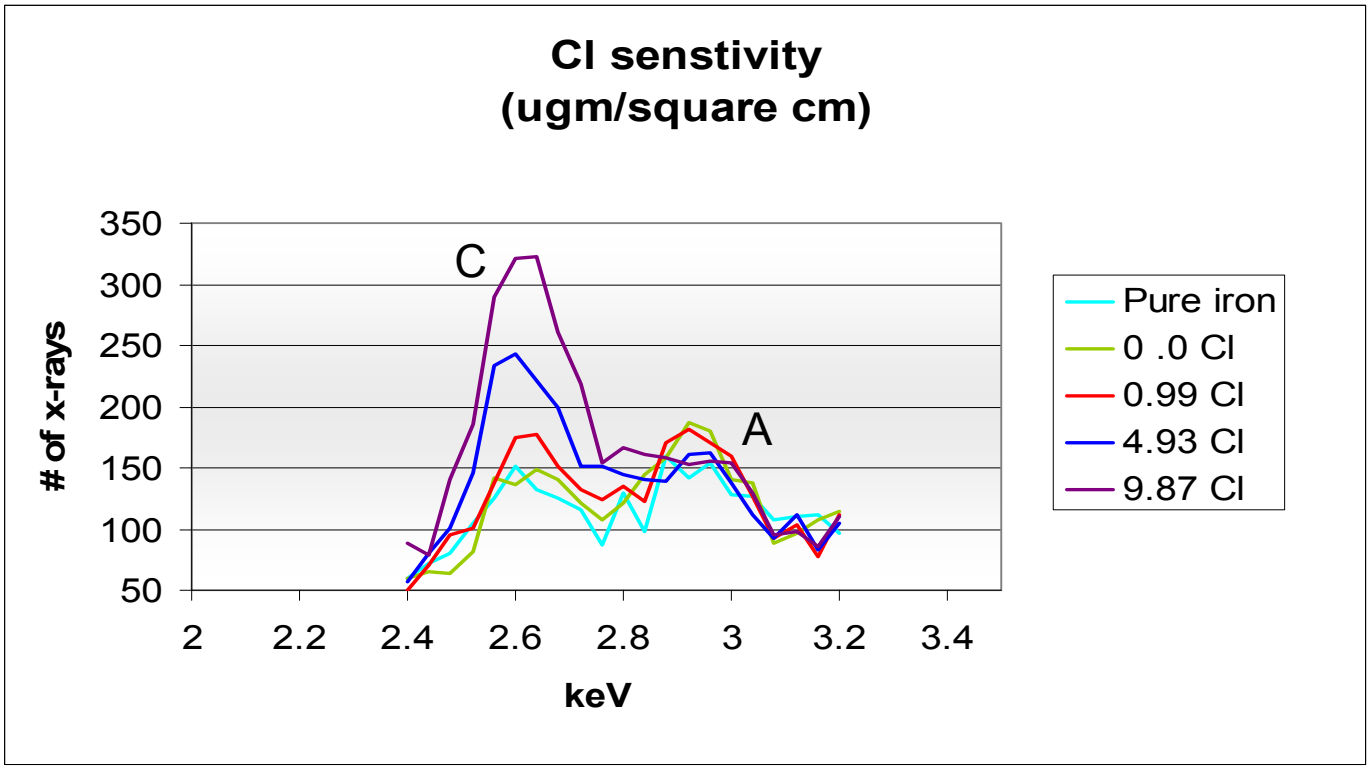

Each standard was analyzed for 3 minutes at 2 different voltage and current settings. A 0.001" Titanium foil was used in both cases to eliminate the Rh L lines and generate Ti x-rays to excite Cl efficiently. The thin paper standards were backed by pure Fe to mimic Cl corrosion on Fe. The above is a plot of the measurements that were taken at 8 kV and 35 micro amps. The peak at 2.6 keV is the Cl K x-ray. The peak at 2.95 keV is a constant amplitude and is a result of Ar K x-ray which is in the air in the paper. It is clear the system is sensitive to Cl down to levels as low as 1 microgram/square cm

Bruker Artax Xrf Scan of Hunley Rivet

The operating parameters are:

- Spot size 0.070 mm2 (micro focus tube)
- Sampling grid 0.070 mm2
- 15 kV tube x ray tube voltage
- Mo tube target
- 300 micro amps x ray tube filament current
- 60 second analysis time per point with Helium flush
- Beam arm was pointed down but can be oriented in
- any direction for any sized object.
- System tripod is on wheels and can be moved quickly.
- Analytical software runs easily on any Windows XP system

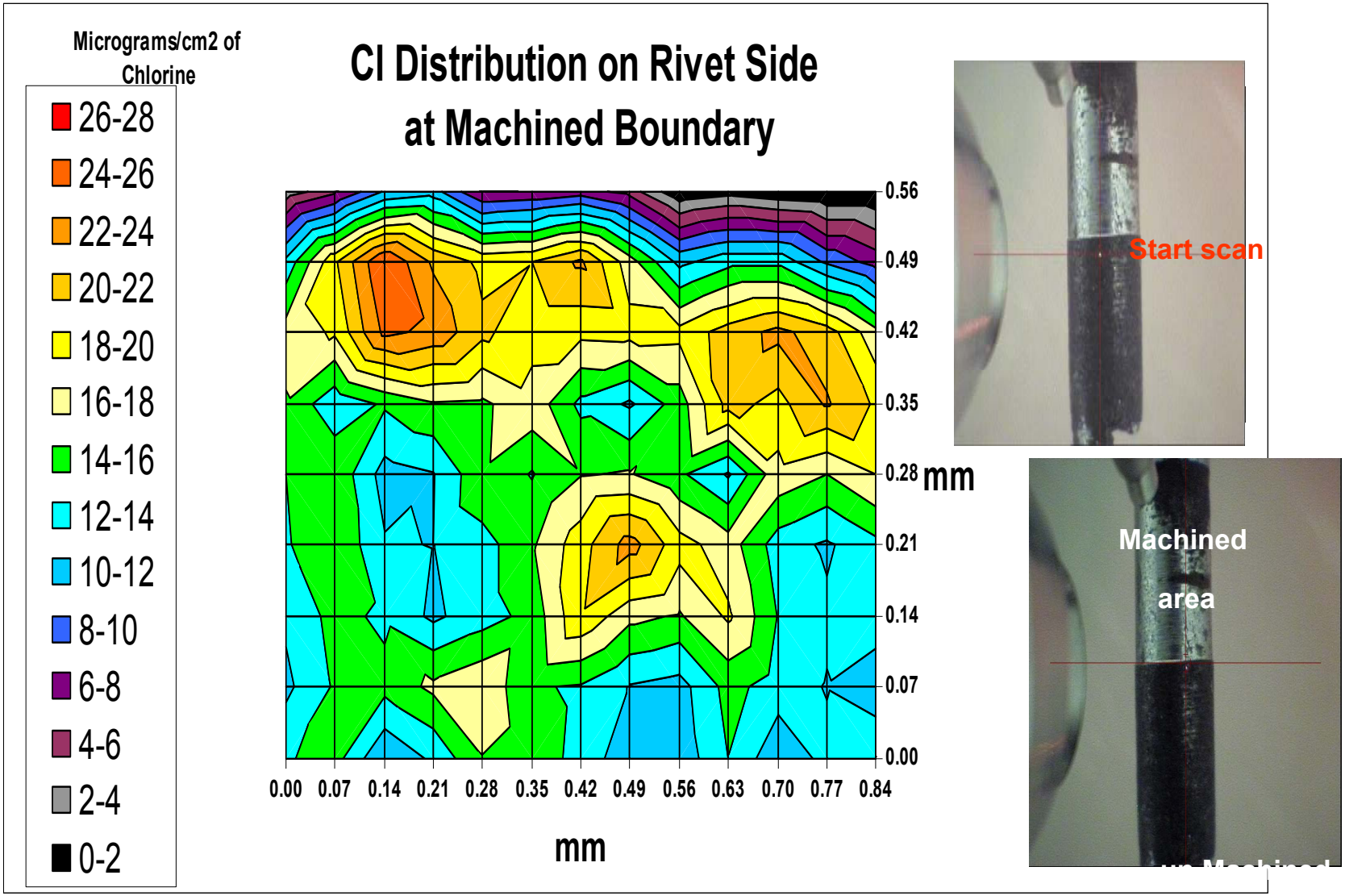
Micrograms/cm2 of Chlorine
26-28
24-26
22-24
20-22
18-20
16-18
14-16
12-14
10-12
8-10
6-8
4-6
2-4
0-2
Cl Distribution on Rivet Side at Machined Boundary
0.56
0.49
0.42
0.35
0.28
0.21
0.14
0.07
0.00
mm
0.00 0.07 0.14 0.21 0.28 0.35 0.42 0.49 0.56 0.63 0.70 0.77 0.84
mm
Start scan
Machined area

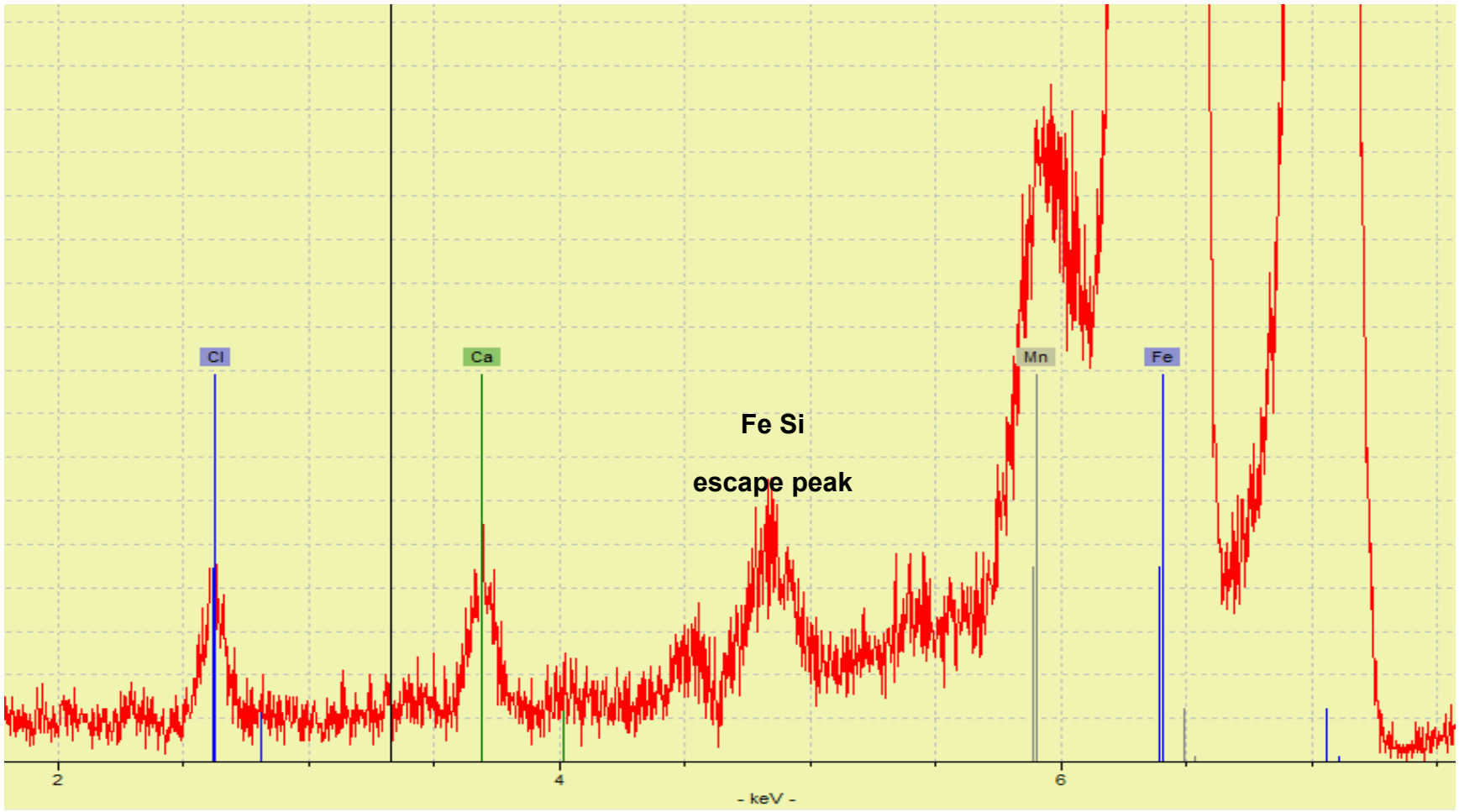

Scan 56 showing typical instrument response

Sourcing Obsidian

- ppm sensitivity to key elements
- Key technique to determine human movement and activity
- Bruker TRACeR xrf systems found to be very accurate for this application
- The following data is an example of Tracer analysis done by Jeff Speakman of the Smithsonian

Bruker TRACeR Operating Parameters

- 40 kV and 10 micro amps
- .006” Cu, .001”Ti, .012” Al filters
- 180 sec data acquisition

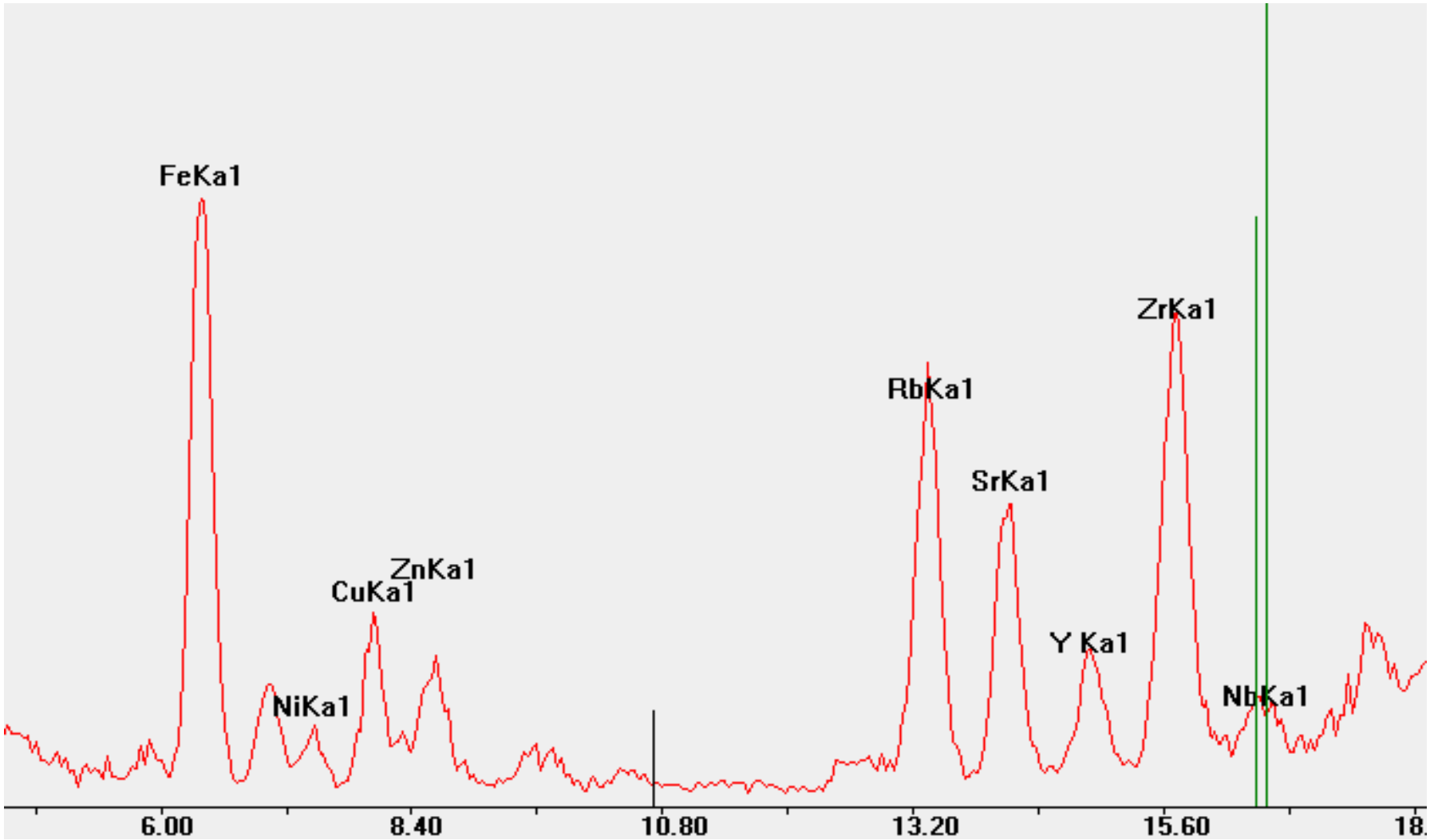
FeKa1
NiKa1
CuKa1
ZnKa1
RbKa1
SrKa1
Y Ka1
ZrKa1
NbKa1
6.00
8.40
10.80
13.20
15.60

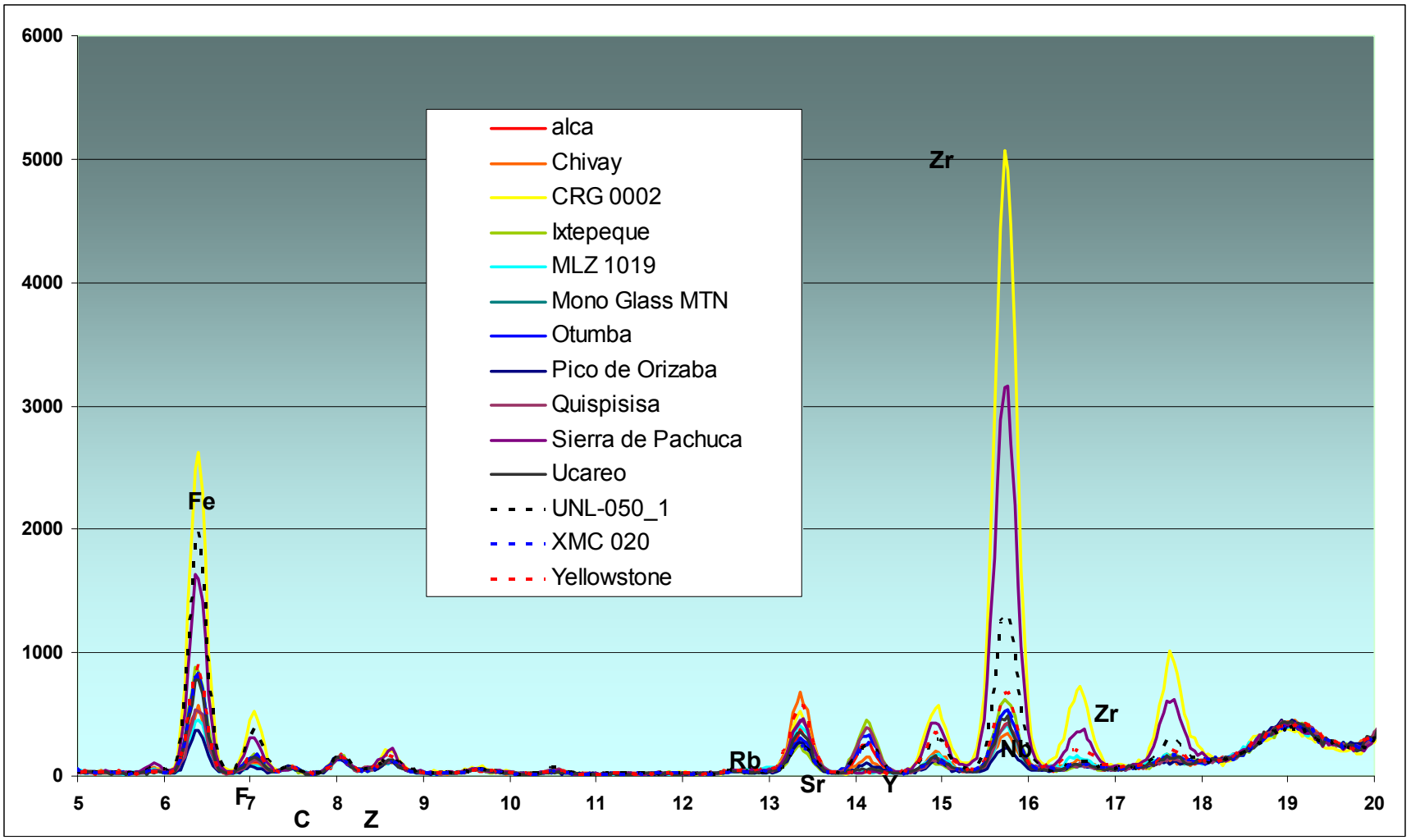
6000
5000
4000
3000
2000
1000
0
5
6
7
8
9
10
11
12
13
14
15
16
17
18
19
20
alca
Chivay
CRG 0002
Ixtepeque
MLZ 1019
Mono Glass MTN
Otumba
Pico de Orizaba
Quispisisa
Sierra de Pachuca
Ucareo
UNL-050_1
XMC 020
Yellowstone
Fe
F
C
Z
Rb
Sr
Y
Zr
Nb
Zr

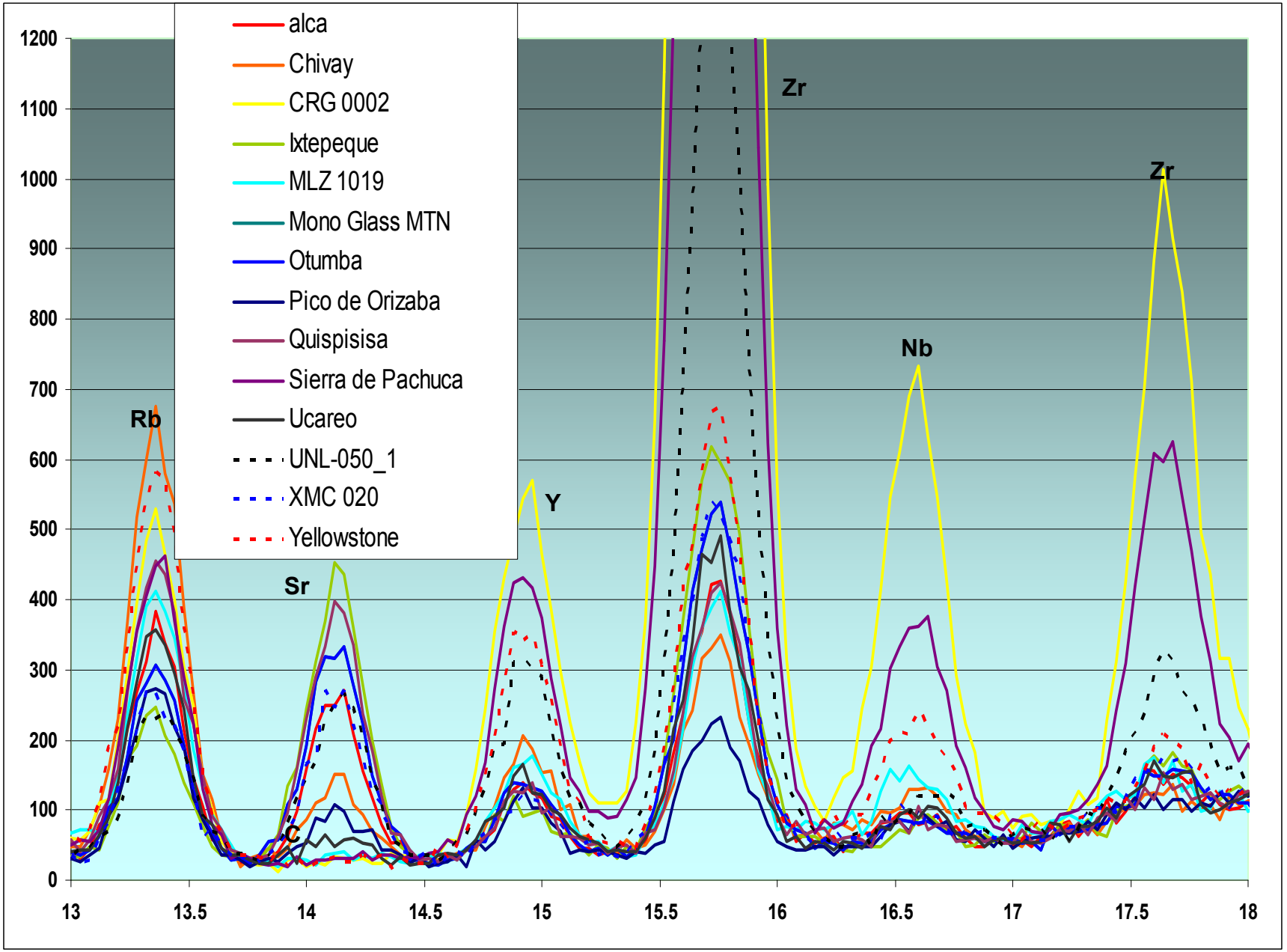
alca
Chivay
CRG 0002
Ixtepeque
MLZ 1019
Mono Glass MTN
Otumba
Pico de Orizaba
Quispisisa
Sierra de Pachuca
Ucareo
UNL-050_1
XMC 020
Yellowstone
Rb
Sr
Y
Zr
Nb
Zr
1200
1100
1000
900
800
700
600
500
400
300
200
100
0
13
13.5
14
14.5
15
15.5
16
16.5
17
17.5
18

Measurement of Toning Agents on Photographs

- Use .006” Cu, .001 Ti, .012” Al filter
- Analyze at photograph
  - 40kV
  - 6 micro amps(what is available)
  - No vacuum
  - 5 to 10 min in
    - White area where there in no toner
    - Areas tone varies grey to black
- Take the difference (toned – white) see below
- The difference will give you a very good clean spectrum of the toning agent. And the grey to black variation will give you an estimate of the amount of agent. The reason this works so well are
  - The toning materials are very thin and have very little effect on the spectrum from the paper
  - The white area is just the paper and mounting materials
  - The filter used removes most of the backscattered x rays

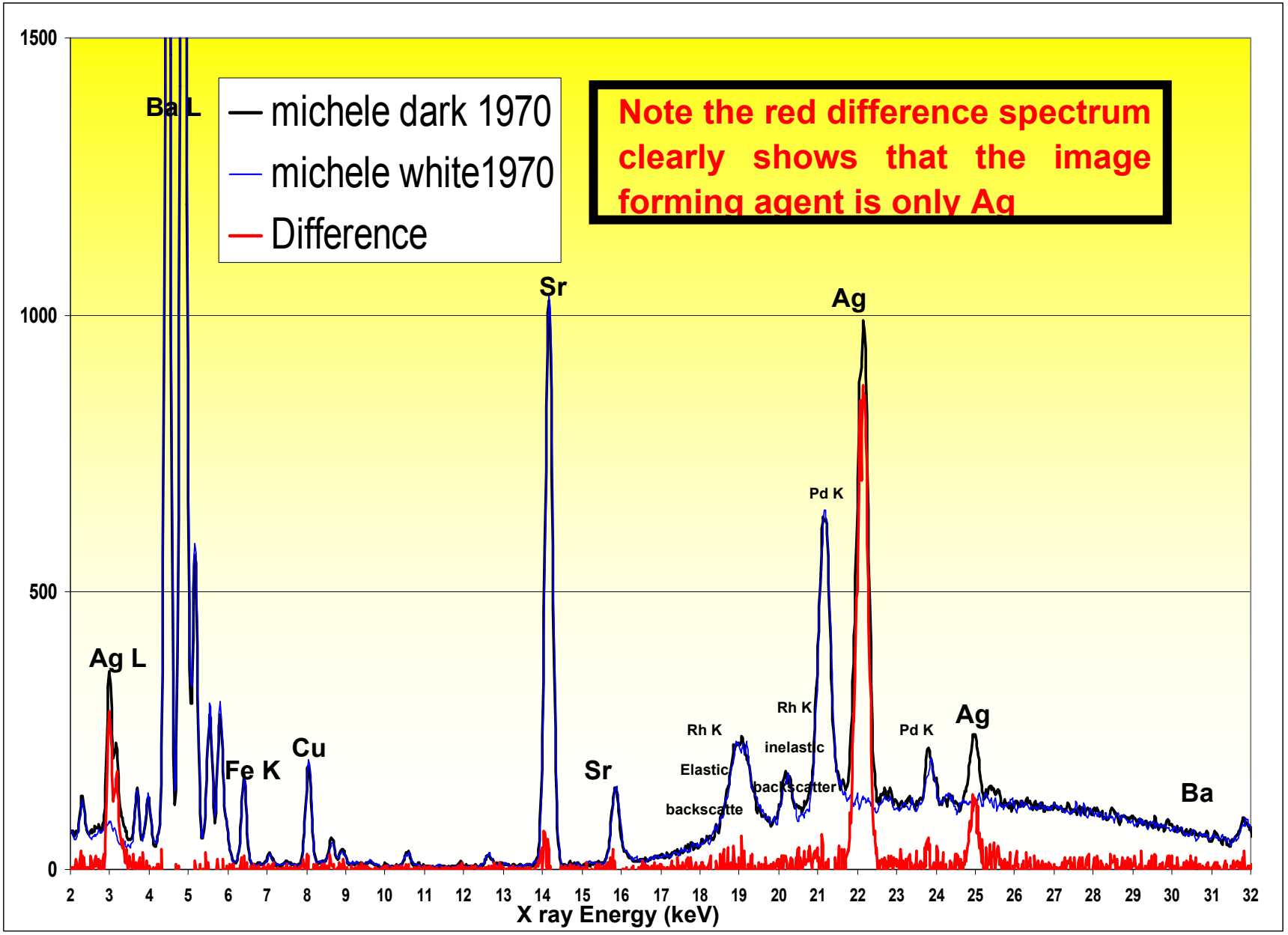
michele dark 1970
michele white1970
Difference
Note the red difference spectrum clearly shows that the image forming agent is only Ag
Ba L
Ag L
Fe K
Cu
Sr
Sr
Rh K
Elastic
backscatte
Rh K
inelastic
backscatter
Pd K
Ag
Pd K
Ag
Ba
1500
1000
500
0
2 3 4 5 6 7 8 9 10 11 12 13 14 15 16 17 18 19 20 21 22 23 24 25 26 27 28 29 30 31 32
X ray Energy (keV)

APPENDICES

APPENDIX A

FILTERS AVAILABLE FOR THE ARTAX AND TRACER UNITS (**NOTE USER CAN MAKE UP ANY FILTER OR SECONDARY TARGET HE CHOSES DEPENDING ON HIS PARTICULAR NEED AND APPLICATION**)

- Some of the Filters available for the ARTAX unit from Bruker
  - 315 µm Al
  - 25 µm Ni
  - 12.5 µm Ni
  - 12.5 µm Mo
  - 100 µm Al
  - 200 µm Al

- Some of the Filters available for the TRACeR unit from Bruker
  - Blue filter (1 mil Cu)
  - Yellow filter (12 mil Al + 1 mil Ti)
  - Red filter (12 mil Al + 1 mil Ti + 1 mil Cu)

EFFECT OF A FILTER ON AN X-RAY TUBE SPECTRUM

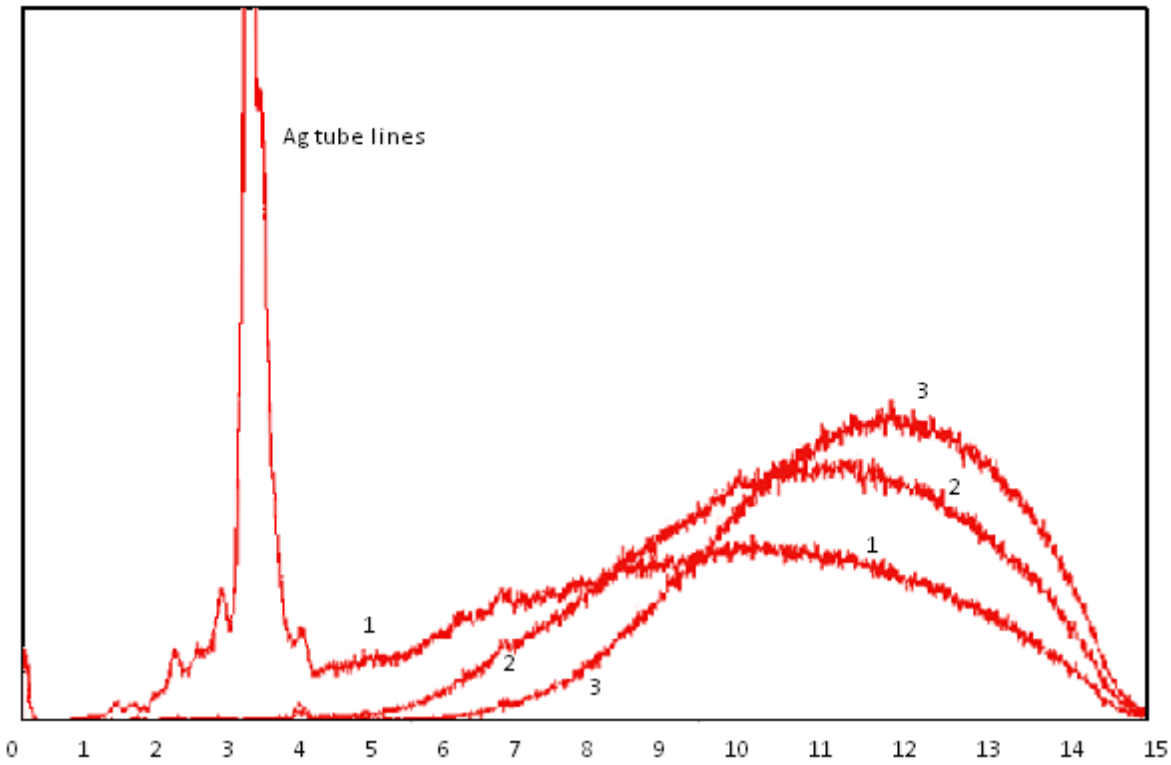

Figure 44: Scattered excitation spectrum provided by a silver target x-ray tube operated at 15 kV. The plots show the effect of two thicknesses of an al primary beam filter: (1) unfiltered; (2) thin al filter; (3) thick al filter.

EXAMPLE OF AN ATTENUATION GRAPH FOR A FILTER COMPOSED OF VARIOUS THICKNESSES OF FE

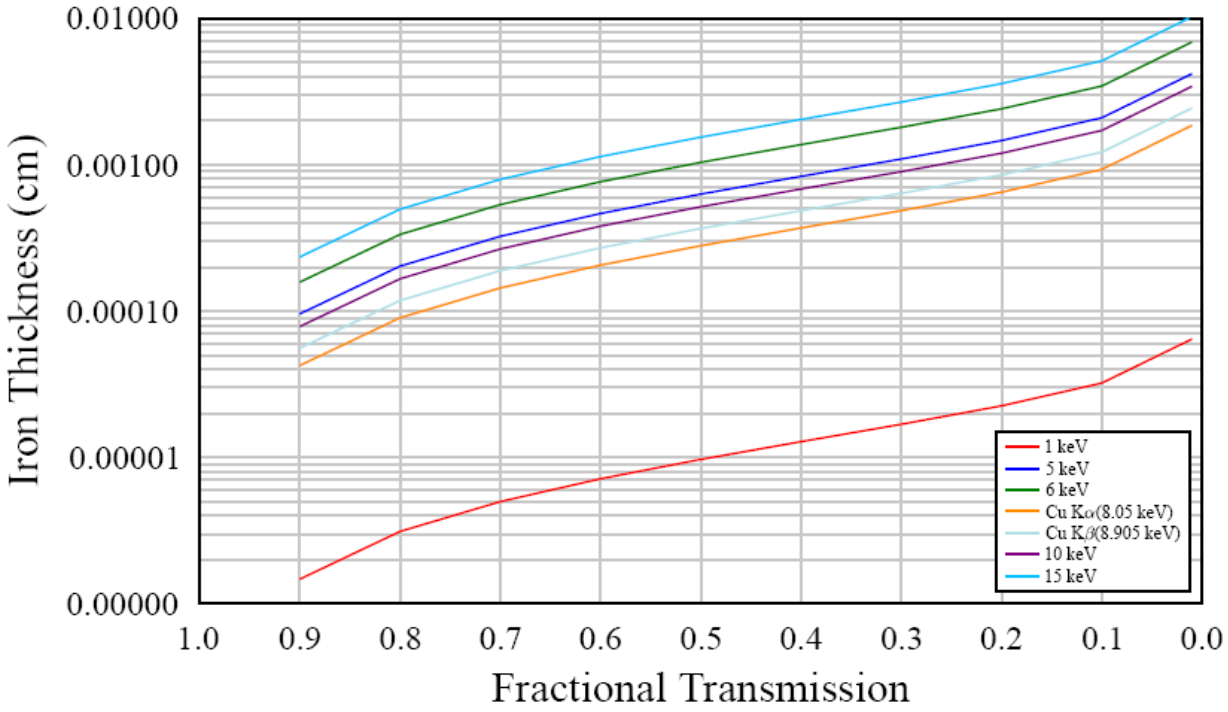

Figure 45: To attenuate a higher percentage of radiation, as well as a higher energy radiation, the filter thickness must increase.

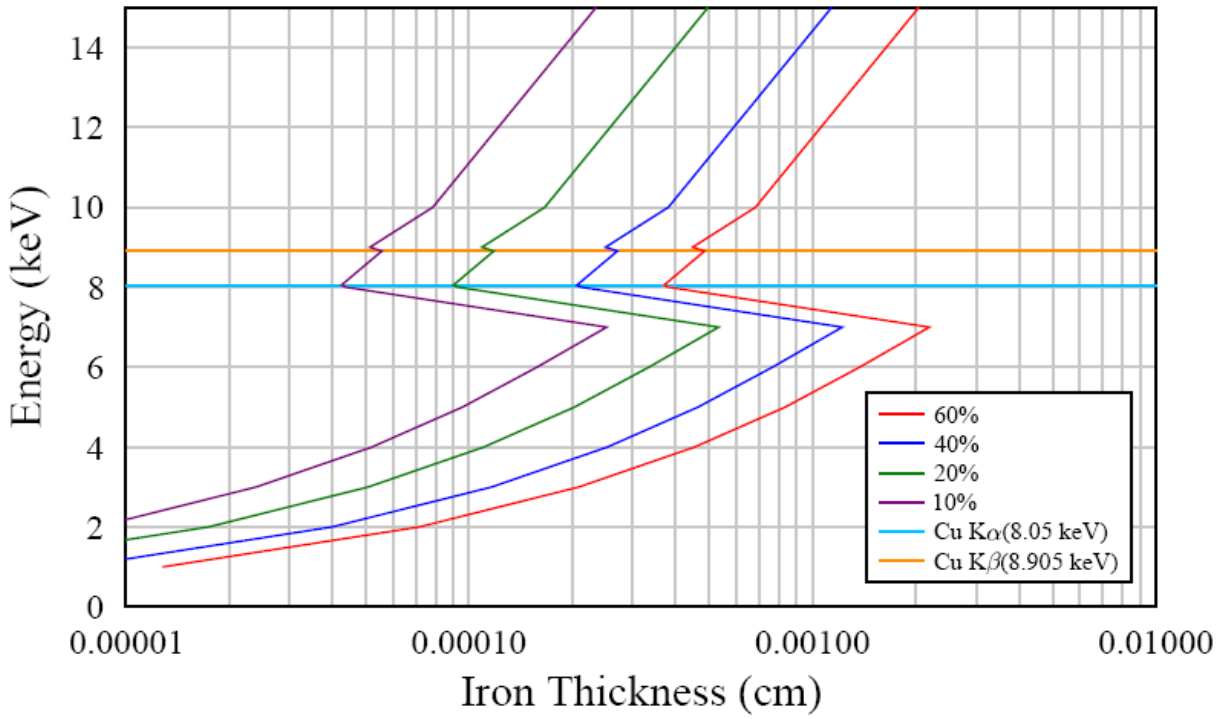

Figure 46: This graph is made to determine the filter thickness required for optimal results in testing a copper sample.

Typical Filter, Voltage and Current Selection For Optimum XRF Elemental Group Analysis using the Tracer

Screening for all Elements (Lab Rat mode):

1. No filter
2. 40 kV
3. 3 to 5 micro amps (for non metallic samples)
4. 0.6 to 1.4 micro amps (for metallic samples)
5. Utilize the vacuum.

These settings allow all the x rays from 1 keV to 40 keV to reach the sample thus exciting all the elements for Mg to Pu.

To optimize for particular elemental groups one wants to use filters and settings that "position" the X ray energy impacting the sample just above the absorption edges of the element(s) of interest. Examples of how to go about this is given below. Note as well that the depth of analysis is also very much a function of both the x ray energy used to probe the material and the element that is being excited, both are exponential functions dependent on the matrix of elements that the material is composed.

Measurement of Obsidian for higher Z elements (Rb, Sr, Y, Zr, and Nb):

1. 0.006” Cu, .001” Ti, .012 Al Filter
2. 40 kV
3. 4 to 8 micro amps
4. No vacuum

These settings allow all the x rays from 17 keV to 40 keV to reach the sample thus efficiently exciting the elements from Fe to Mo. These are some of the key elements to identifying the origin of the obsidian and many other natural occurring materials used by early man. There is little or no sensitivity to elements below Fe with these settings.

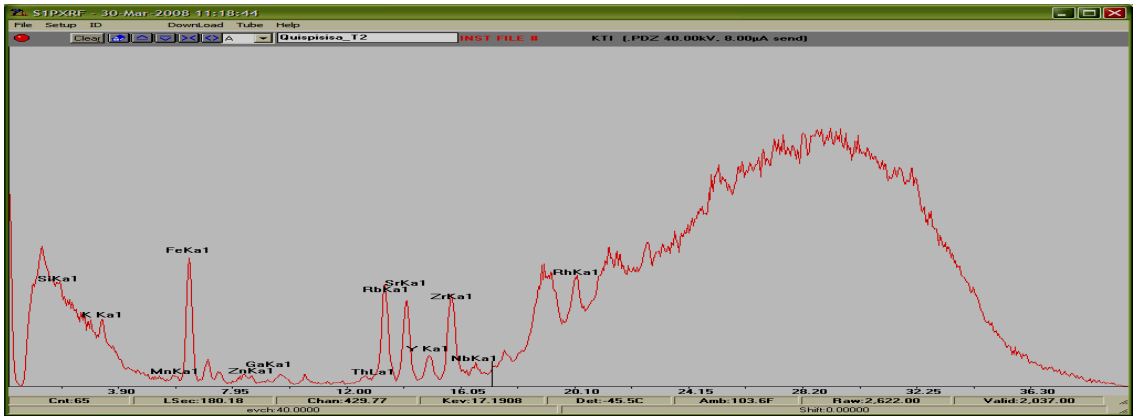

Measurement of Mg, Al, Si and P to Cu(and any L and M lines for the elements that fall between 1.2 and 8 keV)

1. No filter
2. 15 kV
3. 15 micro amps
4. Vacuum

These settings allow all the x rays from the tube up to 15 keV. In particular this allows the Rh L(2.5 to 3 keV) lines from the tube to reach the sample. These are particularly effective at exciting the elements with their absorption edge below 2.3 keV. Note this set up is not good for Cl and S detection, as the scattered Rh L lines interfere with the x rays coming from these elements.

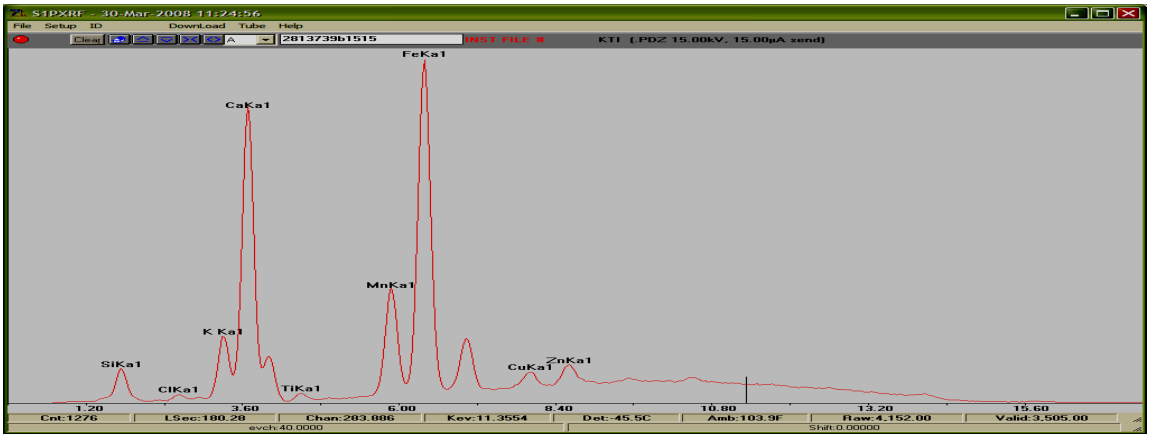

Measurement of Mg, Al, Si, P, Cl, S, K, Ca, V, Cr, and Fe (and any L and M lines for the elements that fall between 1.2 and 6.5keV)

1. Ti filter
2. 15 to 20 kV
3. 15 to 20 micro amps
4. Vacuum

These settings allow x-rays from 3 to 12 keV to reach the sample. In particular this does not allow the Rh L lines from the tube to reach the sample. These Rh L x rays would interfere with Cl and S analysis. For example, this is a very good set up for measuring Cl on the surface of Fe.

Measurement of metals (Ti to Ag K lines and the W to Bi Lines):

1. 0.001" Ti, .012 Al Filter (yellow)
2. 40 kV
3. 1.2 to 2.6 micro amps
4. No vacuum

These settings allow all the x rays from 12 keV to 40 keV to reach the sample thus efficiently exciting the elements noted above. These are the settings used to calibrate the system for all modern alloys of those elements of those listed in the title of this section. There is little or no sensitivity to elements below Ca with these settings.

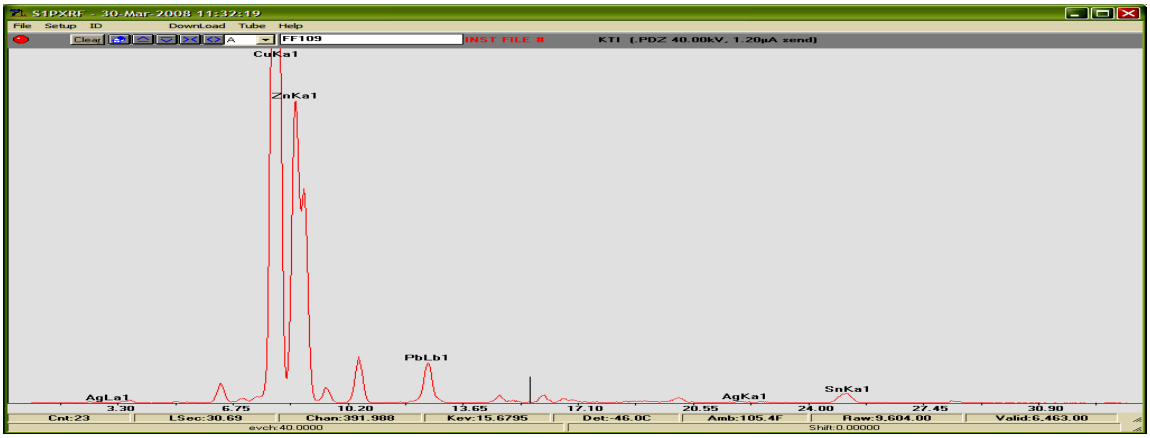

Measurement of Poisons (higher Z elements Hg, Pb, Br, As):

1. 0.001” Cu, .001” Ti, .012 Al Filter
2. 40 kV
3. 4 to 8 micro amps
4. No vacuum

These settings allow all the x rays from 14 keV to 40 keV to reach the sample thus efficiently exciting the elements Hg, Pb, Br, As. These are some of the key elements that were used to preserve organic based artifacts. There is little or no sensitivity to elements below Ca with these settings.

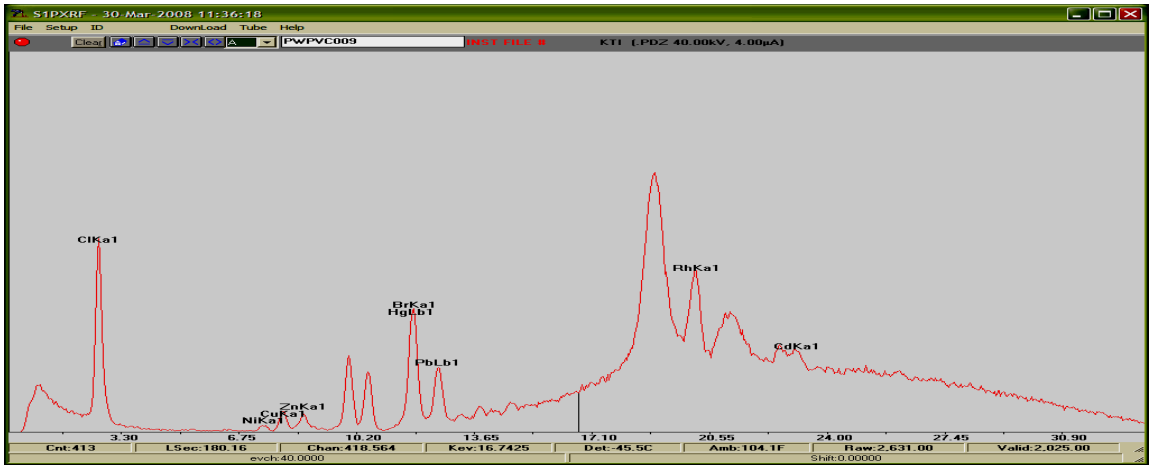

APPENDIX B

Explanation of Material Characteristics

[1] The higher the specific density of the detector material, the better its stopping power for higher energy x-rays (emissions greater than 20 keV). For example, elements such as Cd, Sn, Sb, Ba.

[2] A larger band gap makes the detector less sensitive to thermal noise.

[3] Higher melting point contributes to detector durability and ruggedness.

[4] Harder material is more rugged, easier to handle and machine.

[5] Higher energy requirement per creation of one pair means worse energy resolution.

[6] Higher resistivity means that a higher voltage is required for detector polarization.

[7] Higher mobility, especially that of holes, improves the count rate capability of the detector, energy resolution, and long-term stability(low trapping).

Figure 47: Explanation of Si PIN characteristics

APPENDIX C

Parameter	ARTAX 200	ARTAX 400	ARTAX 800
X-ray tube			
Type	Metal ceramic, air-cooled	Metal ceramic, air-cooled	Metal ceramic, air-cooled
Target	Mo, W, Rh, Cu	Mo, W, Rh, Cu	Mo, W, Rh, Cu
Focal spot	1.2 x 0.1 mm^2	1.2 x 0.1 mm^2	0.05 x 0.05 mm^2
Target angle	6°	6°	12°
Window	100 µm Be	100 µm Be	100 µm Be
max. HV	50 kV	50 kV	50 kV
max. current	1000 µA	1000 µA	600 µA
max. power	50 W	50 W	30 W
X-ray optics			
Type	Collimator	Collimator	Mini-lens, filled with He
lateral resolution [mm]	0.20 mm 0.65 mm 1.00 mm 1.50 mm	0.20 mm 0.65 mm 1.00 mm 1.50 mm	Varies with lens type: e.g. 75 µm for 15-20 keV
Gain	none	none	e.g. 2500 for 15-20 keV
Helium flush			
Type	none	Regulated via flow controller	Regulated via flow controller
Setting	none	via software	via software
Flush	none	Flush of collimator and flush of detector nozzle	Flush between lens and tube, lens and sample, detector nozzle and sample, lens He-filled
Detector			
Type	SDD, peltier cooled	SDD, peltier cooled	SDD, peltier cooled
Area	10 mm^2	10 mm^2	10 mm^2

ARTAX 200 tripod		
Maximum working height: vertical horizontal	 mm / inch mm / inch	 1130 / 445 1560 / 614
Minimum working height: vertical horizontal	 mm / inch mm / inch	 870 / 343 1300 / 512
Transport box: Length Width Height	 mm / inch mm / inch mm / inch	 1200 / 472 580 / 288 370 / 146
Weight	kg	20

Tab. 6: Dimensions and weights of ARTAX 200, 400 and 800

Connection values		
Voltage	V Hz	100–230 V ±10 % 50/60
Maximum power	W	300
Connection	Protective contact plug 1P+N+PE as per DIN 49441	
Operational conditions		
Ambient temperature	°C	10–30
relative humidity (non-condensing)	%	10–80
Ambient air	Free of corrosive vapours Free of large dust exposure	

Parameter	ARTAX 200	ARTAX 400	ARTAX 800
Resolution	<155 eV at 10 kcps	<155 eV at 10 kcps	<155 eV at 10 kcps
max. count rate	>100 kcps	>100 kcps	>100 kcps
CCD Camera			
Type	¼" CCD	¼" CCD	¼" CCD
Active pixel	500 x 582 PAL	500 x 582 PAL	500 x 582 PAL
Sensitivity	<0.5 Lux	<0.5 Lux	<0.5 Lux
Magnification (dependent on monitor)	approx. 20	approx. 20	approx. 20
Signal	Composite	Composite	Composite
Digitalisation	fire wire converter	fire wire converter	fire wire converter
Measuring head angle adjustment			
Type	manual	manual	manual
Range	0 .. 90°	-10° ...100°	-10° ...100°
Resolution	15°	6°	6°
XYZ positioning			
Type	manual	step motor	step motor
Range	Z pos. Manual linear drive ±18 mm, X,Y pos. via tripod	±22 mm	±22 mm
Resolution	50 µm	10 µm	10 µm

Dimensions: Measuring head		
Length Length with cable	mm/inch mm/inch	450/177 500/197
Width	mm/inch	150/59 (ver. 400) 200/79 (ver. 800)
Height	mm/inch	230/91
Weight	kg	5.2
XYZ adjustment unit, ARTAX 400, 800		
Length (X)	mm/inch	280 / 110
Width (Y)	mm/inch	265 / 104
Height (Z)	mm/inch	325 / 128
Weight	kg	8,0
Elektronics unit		
Length (with handle)	mm/inch	590 / 232
Width	mm/inch	345 / 136
Height	mm/inch	210 / 83
Weight	kg	23,1
Transport box 1		
Length	mm / inch	1340 / 136
Width	mm / inch	650 / 256
Height	mm / inch	450 / 177
Total weight	kg	75
Tripod, ARTAX 400 and 800		
Maximum working height: vertical horizontal	 mm / inch mm / inch	 1230 / 484 1650 / 649
Minimum working height: vertical horizontal	 mm / inch mm / inch	 450 / 177 870 / 348
Transport box: Length Width Height	 mm / inch mm / inch mm / inch	 1100 / 433 580 / 67 380 / 150
Total weight	kg	70

APPENDIX D

Beryllium Copper C1122		Phosphorized Cu C1251a	
Elem	%	Elem	%
Sb		Sb	.0014
Sn	.01	Sn	.0016
Ag	.005	Ag	.0080
Bi		Bi	.00037
Pb	.003	Pb	.00235
Se		Se	.0011
Zn	.01	Zn	.0024
Cu	97.45	Cu	99.89
Ni	.01	Ni	.00236
Co	.22	Co	.00132
Fe	.16	Fe	.0285
Mn	.004	Mn	.00046
Cr	.002	Cr	.0003
Al	.17	Al	< .002
P	.004	P	.0420
Si	.17	Si	<.005
Mg		Mg	<.002
S		S	.0035
Be	1.75	Cd	< .0003
As		As	.0016
Te		Te	.0016
Au		Au	.00155

Table 8: Elemental composition of NIST standards C 1122 and C 1251a

APPENDIX E

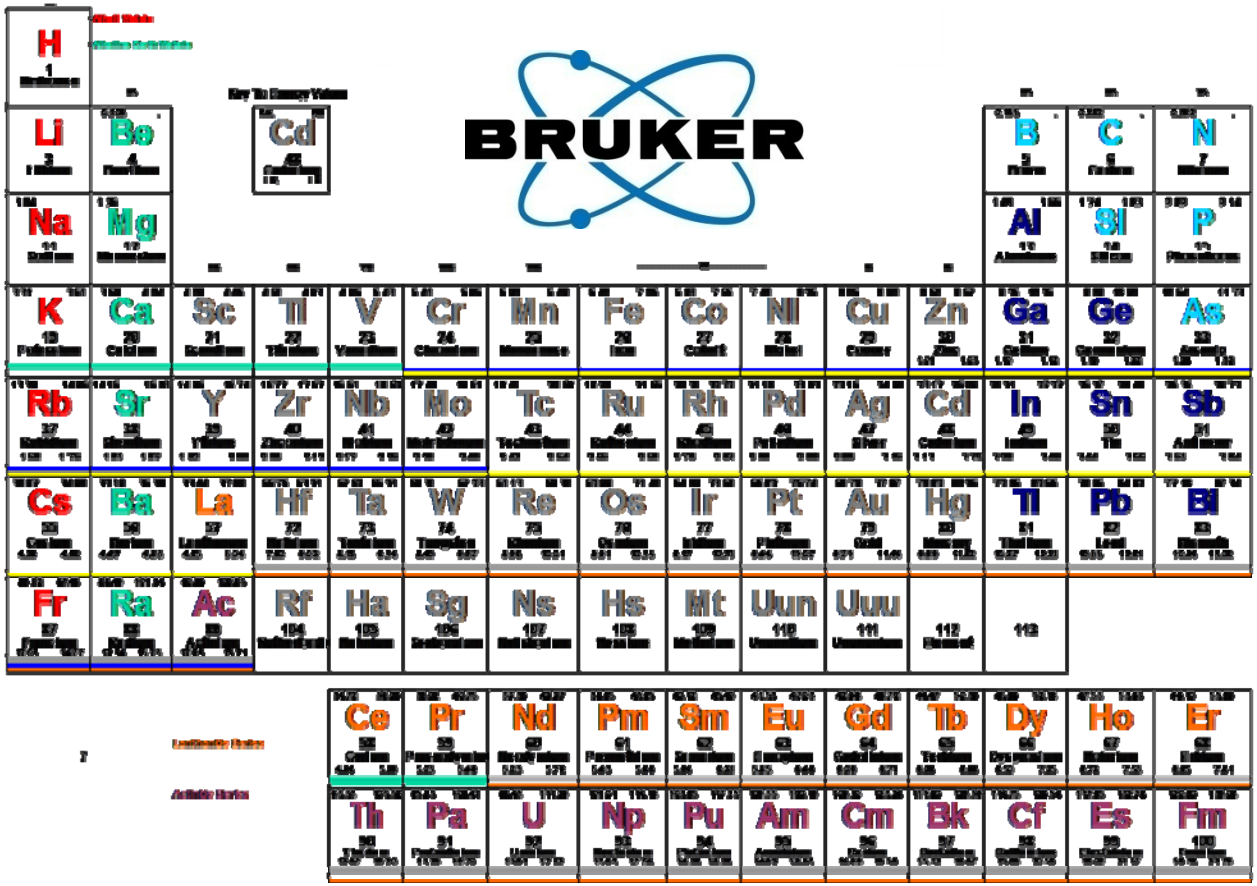

Figure 48: Periodic table including the K and L series characteristic energies of all of the elements